1990

Burial diagenesis in two non-marine Tertiary basins southwestern Montana

Douglas K. McCarty
The University of Montana

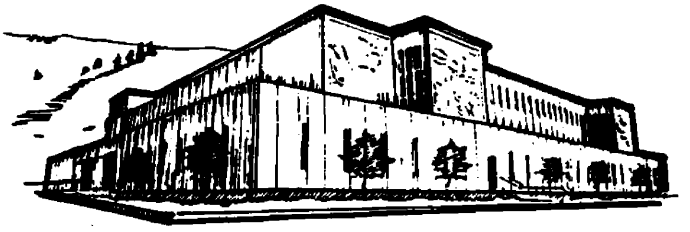

BURIAL DIAGENESIS IN TWO NON-MARINE TERTIARY BASINS, SOUTHWESTERN MONTANA

by

Douglas K. McCarty

B.A. University of Montana, 1986

Presented in partial fulfillment of the requirements

for the degree

Master of Science

University of Montana

1990

Approved by:

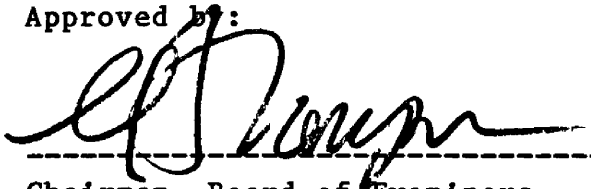

Chairman, Board of Examiners

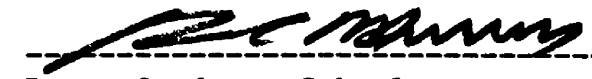

Dean, Graduate School

March 29, 1990

Date

ProQuest LLC.
789 East Eisenhower Parkway
P.O. Box 1346
Ann Arbor, MI 48106 - 1346

McCarty, Douglas K., M.S., January 1990 Geology

Burial diagenesis in two non-marine Tertiary basins, southwestern Montana (73 pp.)

Director: Graham R. Thompson

Samples from initially smectite-rich Tertiary continental volcaniclastics sediments from the Deer Lodge and Big Hole basins of southwestern Montana show a general decrease in illite/smectite (I/S) expandability with increasing burial depth. The mineralogical trends in cuttings samples from seven wells are interrupted by discontinuities in which I/S expandability abruptly decreases by an amount varying from 30 to 80 percent. I/S expandability discontinuities are coincident with stratigraphic unconformities in all four of the wells in which the stratigraphy is known.

Core samples show significant differences from the trends seen in cuttings samples from the same well and from typical marine sequences. A wide range of I/S expandabilities occurs over a short stratigraphic interval in core samples. This variation may be due to composition, porosity, and permeability variations. Sericite coexists with I/S in the deep core samples. The sericite may represent the end product of the illitization of smectite, and the coexisting I/S may have grown after a separate nucleation event. Alternatively, the sericite may be unrelated to an illitization process.

A core sample from 7958 ft. contains an R3 ordered I/S with a nearly ideal 3:1 illite to smectite ratio, similar to the mineral tarasovite. The structure of this I/S is consistent with a sample dominated by stacks of four 2:1 layer fundamental illite particles with small proportions of thicker particles randomly interstratified among the four-layer particles. These data suggest that fundamental particles four 2:1 layers thick with R3 ordering may be metastable or stable.

ACKNOWLEDGEMENTS

Special thanks go to my committee; Gray Thompson, Don Hyndman, and Keith Osterheld for their expert advice and support.

Thanks also to Dennis Eberl for his expertise and enthusiasm, and the U.S. Geological Survey, Denver, CO, for student sponsorship.

This project was partially funded by The Clay Minerals Society Student Research Grant Program, and the University of Montana McDonough Research Grant Program, to whom I am very grateful.

I would also like to thank my fellow student, Jeff Moe, for his generous help in the completion of this project.

TABLE OF CONTENTS

LIST OF FIGURES

LIST OF FIGURES CONT.

Figure Page

LIST OF TABLES

INTRODUCTION.

Low-grade metamorphic (diagenetic) clay mineral reactions are well-documented in deeply buried clay-rich marine sedimentary basins (e.g. Burst, 1959, Dunoyer De Segonzac, 1970, Hower et al., 1976, Jennings and Thompson, 1986). Most commonly, the reactions involve the progressive illitization of smectite, disappearance of kaolinite, and appearance of chlorite, with increasing depth and temperature. No detailed studies have been made to date, however, of clay mineral reactions in deeply buried non-marine Tertiary clay-rich terrestrial sedimentary basins.

It is well known that system composition controls paths and rates of clay mineral reactions in burial diagenetic sequences (Boles and Franks, 1979, Howard, 1987, Eberl and Hower, 1976, Whitney and Northrop, 1988, Huang, 1988). Dutta and Suttner (1986) have shown that climate plays an important role in authigenic clay mineral growth in the pore space of near-surface non-marine sandstones. Compositional differences between interstitial waters in marine and non-marine sediments, and effects of climate and depositional environment in non-marine basins, may result

in mineralogical differences between non-marine and marine sediments during diagenesis. In this paper I describe the clay mineralogy and petrology of two clay-rich Tertiary non-marine basins in southwestern Montana, and compare the clay diagenetic trends with those of marine basins.

GEOLOGIC SETTING.

Several large southwest Montana basins filled with sediment as they developed in response to Tertiary tectonic activity. The dominant sediments of the Deer Lodge and Big Hole basins of southwestern Montana (Figure 1) are assigned to the Renova and overlying Sixmile Creek Formations. Their ages range from late Eocene through latest Miocene. The sediments of both units consist of volcaniclastics initially rich in rhyolitic ash, gravels derived from the immediately adjacent mountain ranges, and organic-rich lake and swamp deposits. The Renova Formation unconformably overlies the clay-rich Lowland Creek Volcanics. In the Deer Lodge basin the Lowland Creek unit unconformably overlies late Cretaceous black shales of the Colorado Group (Figure 2).

The Sixmile Creek and Renova formations are commonly separated by an erosional unconformity which in some

localities also shows an angular relationship (Fields et al., 1985). The high organic content in the lacustrine and swamp facies of the Renova Formation, and burial depths in excess of 10,000 feet, have made the Tertiary basins of southwestern Montana targets for petroleum exploration during the past 10 years.

ANALYTICAL METHODS.

Sampling.

Samples were taken from cuttings and cores collected by AMOCO Production Company from two exploratory wells in the Big Hole Valley, and from five wells in the Deer Lodge Valley (Figure 1). Cuttings samples were collected at 100-200 foot intervals from each of the five Deer Lodge Valley wells, and at 30 foot intervals from the two Big Hole Valley wells. Core samples were taken from those sections of the two Big Hole valley wells that were cored.

Sample treatment.

All samples were washed in deionized water to remove drilling mud contamination. Samples were crushed in a glazed porcelain mortar and disaggregated in deionized water with an ultrasonic probe. In the cuttings samples, <0.5 micron (equivalent spherical diameter) size fractions

were separated from <2.0 micron size fraction suspensions for X-ray diffraction (XRD) analysis by centrifugation. In the core samples from the Hirshey #2 well in the Big Hole Valley the <0.5 micron and <0.1 micron size fractions were separated from <2.0 micron clay suspensions by centrifugation.

All clay samples were strontium saturated to eliminate variations in glycol thickness caused by large monovalent cations (Eberl et al., 1986). The samples were subsequently washed to remove excess electrolyte.

X-ray diffraction analysis.

Oriented samples of the various size fractions were prepared for XRD analysis by a filter-membrane peel technique (Pollastro, 1982).

XRD analyses were made of all oriented samples from 2 to 50 degrees two-theta, and for selected samples from 2 to 90 degrees. Samples were run on a Philips X-ray diffractometer with a digital step counter using copper K alpha radiation and a graphite crystal-monochromator. Some samples were analyzed with an automated Siemens D500 diffractometer.

All oriented samples were analyzed by XRD after glycol solvation in a heated solvation chamber for 24 hours. Some of the samples were analyzed in the air-dried state for comparison with glycol solvated XRD patterns.

Selected oriented samples were heat treated at 600 degrees C for one hour and then analyzed by XRD to determine the presence of kaolinite (Carroll, 1970).

Illite/smectite (I/S) identifications were made using techniques of Srodon (1980, 1981, 1984), Reynolds and Hower (1970) and the NEWMOD computer program (Reynolds, 1985).

Scanning-electron microscope analysis (SEM).

Chips from selected Hirshey #2 core samples were cemented onto aluminum mounts, sputter-coated with Au-Pd alloy, and in some cases carbon. The mounted samples were examined with a Cambridge Stereoscan 250 MK2 SEM at 20 kv for textural indications of authigenic clay growth. Identification of clay minerals was aided by a spot specific Energy Dispersive X-ray Spectrum (EDX) chemical analyzer.

Optical microscopy.

Standard thin sections were cut from selected core samples from the Hirshey #2 well and examined under the

optical microscope to observe whole rock textural characteristics and replacement textures.

RESULTS.

Mineralogical results.

The dominant mineral in the clay size fraction from the cuttings and core samples from all seven wells is illite/smectite (I/S). The clay mineralogy of cuttings and core samples from each well is summarized in Tables 1 through 9, and Figures 3 through 11. The expandabilities of I/S from cuttings samples are plotted against depth for the <0.5 micron fraction in Figures 3-9 to show mineralogical trends for each well.

Cuttings samples.

The Benson Well (Figure 3; Table 1) contains R0 I/S from 1500 ft. to the bottom of the hole at 7100 ft. The I/S is 100 percent expandable to a depth of 6000 ft. where the expandability abruptly decreases to 50 percent. The deepest samples at 6700 ft. and 7100 ft. are both 40 percent expandable. Most of the samples also contain discrete illite and chlorite or kaolinite.

The Arco Well (Figure 4; Table 2) contains R0 I/S from 1000 ft. to the bottom of the hole. The I/S expandability

varies somewhat erratically with depth, but is greater than 80 percent to 5700 ft. where it abruptly decreases to 50 percent. It remains at 50 percent to the bottom of the hole. Below 2900 ft. chlorite or kaolinite were also present. Discrete illite is present in samples below 2900 ft.

In the Lewis Johnson Well (Figure 5; Table 3), highly expandable R0 I/S is present to a depth of 7400 ft. The samples from 8000 ft. to 9000 ft. show an ordering and expandability transition between highly expandable R0 I/S and R1 I/S of lower expandability. Neither the ordering or the expandability could be precisely identified from the XRD patterns in this depth range, but expandability is estimated at 50 percent. Below these samples, at 9500 and 9700 ft., R1 ordered I/S exists with expandabilities of 30 percent and 25 percent respectively. R3 ordering occurs at 9800 ft. in I/S with 18 percent expandability. The deepest sample at 9900 ft. shows R3 ordering with 16 percent expandability. Chlorite or kaolinite and discrete illite coexist with I/S in most of the samples.

In the Jacobson Well (Figure 6; Table 4), highly expandable R0 I/S exists from 1000 ft. to 5500 ft. At 6000

ft. there is an abrupt mineralogical discontinuity below which all samples to the bottom of the hole at 11000 ft. contain illite with no measurable expandability and chlorite.

In the Montana State Prison Well (Figure 7; Table 5), a discontinuity similar to that in the Jacobson well exists between highly expandable R0 I/S, and illite with no measurable expandability, but the abrupt transition occurs at a depth of 2000 ft. Discrete illite coexists with all R0 I/S. Chlorite and/or kaolinite coexist with the illite samples down to 3000 ft. From 3500 ft. to the bottom of the hole at 6300 ft. chlorite coexists with illite.

In the Hirshey #1 Well (Figure 8; Table 6), from 300 ft. to 6140 ft. 100 percent expandable R0 I/S coexists with discrete illite and chlorite. An abrupt mineralogical discontinuity occurs between 6140 ft. and 6560 ft. From 6560 ft. to 15790 ft. I/S expandability decreases from 32 percent to nearly zero. From 6560 ft. to 11440 ft. ordering of most samples is intermediate between R1 and R2 (designated R1/R2). R1/R2 I/S ordering is identified on the basis of XRD between reflections 20 and 37 angstroms, and criteria described by Srodon (1980, 1981, 1984).

Chlorite coexists with I/S in most of the samples in this zone. R3 ordering begins with the 13960 ft. sample and persists to the bottom of the hole at 15790 ft.

In the Hirshey #2 Well (Figure 9; Table 7), expandability generally decreases from 100 percent to 10 percent from 2000 ft. to 13000 ft. Ordering of I/S is R0 from 2000 ft. to 6200 ft. Ordering of the R1/R2, R1, and R3 types exists without a trend from 6000 ft. to 13000 ft. Chlorite is present as an accessory mineral in all samples from 4500 ft. to the bottom of the hole. Discrete illite is present from 4500 ft. to 6600 ft.

Core samples.

Thirty-two core samples from the Hirshey #2 Well were analyzed for clay mineralogy in the interval 6564 ft. to 11883 ft. The core was not continuous over this interval. Many of the samples were stratigraphically closely spaced and no core samples were available between 9049 ft. and 10982 ft. Mineralogical profiles of the <0.5 micron and <0.1 micron size fractions are shown in Figures 10 and 11 and Tables 8 and 9 respectively.

In the Hirshey #2 Well <0.5 micron core samples (Figure 10; Table 8), expandability decreases irregularly from 40

percent to five percent, from 6564 ft. to 7958 ft.. Most of the expandability decrease occurs over a range of only about 300 ft. Ordering is R1/R2 from 6564 ft. to 7590 ft. Chlorite was detected in all samples within this interval. Samples at 7589 ft. and 7590 ft. show distinct feldspar peaks, but the type of feldspar could not be determined. At 7889 ft. R3 ordered I/S occurs and persists to a depth of 9049 ft. Chlorite was detected in only one R3 sample, and feldspar was present in several samples.

At a depth of 10982 ft. the mineralogic character of the core changes significantly. In the XRD patterns from 10982 ft. to the bottom of the hole, very sharp 10 angstrom and integral higher order reflections, are superimposed upon I/S peaks. This 10 angstrom phase will be referred to as sericite for reasons that will be discussed later in the paper. Random powder analyses of the 11873 and 11874 ft. core samples show that the sericite is a mixture of 1m and $2m_1$ polytypes. Expandability of the I/S varies in an irregular manner throughout this interval, but is generally higher than that in the R3 interval above. Expandabilities are as high as 30 percent for R1/R2 ordered I/S, and as low as 12 percent for R3 I/S. R1, R1/R2, and R3 ordering of

I/S are found in this interval. In all samples from 10982 ft. to 11883 ft., chlorite and feldspar are present.

The Hirshey #2 Well, <0.1 micron core samples (Figure 11; Table 9), show a similar profile to that of the <0.5 micron samples. The major difference is that I/S expandabilities average five percent higher in the <0.1 micron size fraction.

Figure 12 shows three examples of XRD patterns from the 6565 to 7590 ft. R1/R2 interval and corresponding NEWMOD (Reynolds, 1985) calculated patterns.

Figure 13 shows three examples of XRD patterns and corresponding NEWMOD (Reynolds, 1985) patterns from the 7889 ft. to 7958 ft. interval. Two of the experimental patterns are R3 ordered, one is R1/R2 ordered.

XRD patterns from the 7958 ft. sample (Figure 14), indicate that the R3 I/S has a nearly ideal I to S ratio of 3:1, based on the presence of a 47 angstrom reflection, and higher order reflections. This type of I/S has been called "tarasovite" by previous workers (Lazarenko, 1949, 1965; Lazarenko and Korolev, 1970; Brindley and Susuki, 1983) and is discussed later in this paper.

I/S in samples from 10982 ft. to 11883 ft. ranges from 16 to 30 percent expandable. All samples from 9049 ft. to 11883 ft. contain sericite. Ordering of the I/S in this lower interval is dominantly R1/R2, but R3 and R1 I/S also exist. Three examples of XRD patterns from this interval are shown in Figure 15, along with corresponding NEWMOD (Reynolds, 1985) calculated patterns. Chlorite and feldspar are also present in most of these samples. I/S peaks are more intense relative to sericite in the <0.1 micron fraction than they are in the larger size fraction.

Mineralogy of different size fractions from single samples.

The relationships among size fraction, I/S expandability, and ordering for the Hirshey #2 well 11000, 10982, and 11872 ft. core samples are shown in Table 10. I/S expandability consistently increases with decreasing size fraction, with the exception of the <0.03 micron size fraction from the 11000 ft. sample (Table 10).

Scanning electron microscopy (SEM).

Figure 16 shows typical examples of mineral textures observed with SEM. Figure 16a is from the Hirshey #2 core sample at 10982 ft.; the curled and delicate texture of the

clay indicates authigenic growth. The high potassium content indicated by the EDX spectrum (Figure 17a), suggests that the clay is illite.

Figures 16b, c, and d are from the Hirshey #2 core sample at 7902 ft. Figure 16b shows authigenic illite laths, based on texture and EDX data (Figure 17b), on the surfaces of authigenic quartz crystals.

Figure 16c shows a mat of authigenic illite, based on EDX data (Figure 17c), with authigenic quartz crystals. The quartz in Figures 16b and 16c is interpreted to be authigenic on the basis of size and euhedral morphology.

Figure 16d shows authigenic quartz, based on EDX data (Figure 17d) and euhedral morphology, with coatings of authigenic clay on the quartz surface.

Figure 16e from the Hirshey #2 11393 core sample, shows apparently authigenic K-feldspar based on EDX data (Figure 17e), size, and euhedral morphology.

Optical microscopy.

Figure 18, shows five photomicrographs illustrating typical rock fabric, and replacement textures from Hirshey #2 well core samples.

Figure 18a, from the 6565 ft. level, shows a sedimentary rock fragment with minor carbonate alteration, in a matrix of unaltered tuffaceous material.

Figure 18b, from the 7890 ft. level, shows tuffaceous clay with a few clasts, and little or no replacement texture.

Figure 18c, from the 11363 ft. depth, shows sericite replacing quartz, and growing outward from the quartz grain. Figure 18d, from the 11363 ft. depth, shows birefringent sericite replacing clastic grains and tuffaceous matrix, and carbonate replacement of a plagioclase grain.

Figure 18e, from the 11363 ft. depth, shows sericite replacement of clastic grains and matrix, with a large white mica that may be authigenic or detrital.

DISCUSSION.

Diagenetic trends in marine sediments generally exhibit a regular progressive decrease in I/S expandability, and an increase in long range ordering with increasing burial depth and temperature (e.g. Hower et al., 1976; Jennings and Thompson, 1986; Velde et al., 1986). The same general trends are seen in the cuttings samples from the Deer Lodge

and Big Hole Valley wells. However, the general mineralogical trends in these wells are interrupted by discontinuities in which I/S expandability abruptly decreases by an amount varying from 30 to 80 percent.

Core samples from the Hirshey #2 well show significant differences from the trends seen in cuttings samples and from typical marine sequences.

Cuttings samples.

Unconformities are well documented in the Tertiary sedimentary section of southwest Montana (Kuenzi and Fields, 1971; Robinson, 1967; Fields et al., 1985). In his study of the depositional history of the Deer Lodge basin, McLeod (1987) correlated stratigraphy between the Lewis Johnson, Benson, Arco, and Jacobson wells based on dipmeter logs, changes in the electrical properties of the rocks, paleontological, and seismic reflection data (Hanson, 1983). Table 11 compares the depth of the I/S discontinuities in the five Deer Lodge Valley wells and two Big Hole Valley wells, with the depths and types of stratigraphic unconformities documented by McLeod (1987). The mineralogic discontinuities coincide with stratigraphic unconformities in all four wells in which stratigraphic

unconformities have been identified.

Two types of mineralogic discontinuities occur in the basins: 1) an abrupt transition from highly expandable R0 I/S to pure illite coexisting with chlorite and 2) an abrupt transition from I/S with high expandability to I/S with lower expandability.

The type 1 discontinuity in the Jacobson well coincides with the boundary between the Tertiary Lowland Creek Volcanics and Cretaceous Colorado Group shale. The Lowland Creek Volcanics are known to be rich in rhyolitic ash, tuffs, and clay-rich volcanic sediments (Iagmin, 1972), which commonly alter to smectite (Moore and Reynolds, 1989). The Colorado Group shale is known to be rich in illite and chlorite (Ehinger et al., 1965). The identical discontinuity seen in the Montana State Prison well may imply a similar Tertiary/Cretaceous contact, although the stratigraphy of that well has not been identified (McLeod, 1987).

In three of the remaining five wells, the mineralogic discontinuities coincide with stratigraphic unconformities between Sixmile Creek Formation and either Renova Formation or Lowland Creek Volcanics. In the other two wells the

depths' of those unconformities are unknown. Studies by other workers have shown that system composition can greatly enhance or inhibit the illitization process (e.g. Eberl and Hower, 1976; Whitney and Northrop, 1988; Huang, 1988). Other studies have shown that permeability variations controlled by rock fabric, control the migration of interstitial fluids and modify system composition, thus affecting the rate and extent of illitization (Boles and Franks, 1979; Howard, 1987). Thus, the coincidence between the I/S discontinuities and stratigraphic unconformities suggests five possible explanations for the mineralogical discontinuities.

1) System composition differences resulting from a change in provenance of the sediments above and below the unconformities may cause the mineralogic discontinuities (Eberl and Hower, 1970; Whitney and Northrop, 1988; Huang, 1988). Significant lithologic and compositional differences are known to exist between the Renova and Sixmile Creek Formations and the Lowland Creek Volcanics (Fields et al., 1985; Iagmin, 1972).

2) Compositional differences in interstitial water, resulting from different permeabilities above and below the

Tertiary unconformities, could differentially effect the illitization process and produce the I/S discontinuities (Howard, 1987; Boles and Franks, 1979). The Sixmile Creek Formation is typically coarser grained than the Renova Formation, which may result in a permeability contrast between the two formations (Fields et al., 1985). The Lowland Creek Volcanics are lithologically different from the Renova and Sixmile Creek Formations and may also show permeability contrasts with those units.

3) System composition differences resulting from climatic differences during the deposition of the sediments above and below the unconformities may cause the mineralogical discontinuities. Climate has been shown to control the bulk composition, and the composition of interstitial waters in clastic sediments (Dutta and Suttner, 1986). The Tertiary sediments in the basins of western Montana contain evidence of major regional climatic variations which are thought to have controlled sedimentation and erosion in the Tertiary basins of western Montana (Thompson et al., 1982).

4) The mineralogical discontinuities may result from a two-stage burial process, interrupted by erosion. The

Renova Formation was deposited in basins which sank progressively from latest Eocene through late middle Miocene time (Fields et al., 1985). In this scenario, illitization of smectite progressed to a significant extent in lower Renova sediments during this first burial event. In late middle Miocene time the Tertiary basins of southwest Montana underwent a period of erosion which removed an unknown thickness of upper Renova sediment (Fields et al., 1985).

The illitization of Lower Renova clays halted or slowed due to this erosion and accompanying cooling. The progressive illitization of smectite is known to be kineticly controlled at temperatures below 300 degrees C. Nevertheless, the rate is affected by temperature (Jennings and Thompson, 1986). Therefore, cooling accompanying erosion would result in cessation or slowing of the illitization reaction. In late Miocene time the Sixmile Creek Formation accumulated on top of the remaining Renova Formation (Fields et al., 1985). As the Sixmile Creek Formation became thicker due to continued deposition, illitization of I/S in the newly reburied Renova Formation recommenced where it left off. At the same time

illitization of smectite-rich sediment of the lower Sixmile Creek Formation began. The head start in development of illite layers gained by the lower Renova Formation during the first burial episode resulted in the current mineralogical discontinuity.

5) The I/S discontinuities may be the result of a combination of these models.

The data do not uniquely support any one of the above models. However, since all of the above processes are known to have affected the Tertiary sediments of southwestern Montana, it seems reasonable that a combination of these effects may be responsible for the pattern of progressive illitization of smectite interrupted by the mineralogic discontinuities coincident with unconformities.

Core samples.

Mineralogical trends with increasing depth in the <0.5 and <0.1 micron fractions (Figures 10 and 11) from the Hirshey #2 core are significantly different from the regular progressive illitization of smectite with depth seen in cuttings samples, described in this study, and from trends seen in cuttings samples in studies of marine

sediments (e.g. Hower et al., 1976; Jennings and Thompson, 1986). Although the Hirshey #2 core samples show a general trend of progressive illitization with depth, they also show wide variations in I/S expandability over short stratigraphic distances, similar to studies by Boles and Franks (1979) and Howard (1987). In addition to these variations the core samples have higher I/S expandability from 9049 ft. to the bottom of the hole than at shallower levels, and these deeper samples coexist with sericite. The mineralogic trends in the Hirshey #2 <0.5 and <0.1 micron fractions are similar to each other except that I/S in the <0.1 micron fraction averages five percent greater expandability than that in the <0.5 micron fraction, and there is a higher proportion of accessory minerals in the <0.5 micron fraction. The following discussion refers to the <0.1 micron fraction samples unless noted otherwise.

The core samples show three distinct mineralogic intervals. Between 6564 ft. and 7590 ft. R1/R2 I/S with expandability from 50 to 32 percent is present (Figure 12). From 7889 ft. to 7958 ft. the samples are comprised of R3 I/S from 26 to 10 percent expandability (Figure 13). From 9049 ft. to the bottom of the hole at 11883 ft. dominantly

R1/R2 ordered I/S of 8 to 30 percent expandability coexists with sericite (Figure 15).

The term sericite is used to indicate highly birefringent, fine-grained, micaceous material as viewed under the optical microscope (Eberl et al., 1987). XRD and microprobe analyses indicate that sericite can have varied structures and compositions (Bonorino, 1959; Shirozu and Higashi, 1972; Le Bel, 1979; Hendry, 1981; Nicot, 1981; Meunier and Velde, 1982; Omelyanenko et al., 1982; Cathelineau, 1983; Beaufort and Meunier, 1983; Horton, 1983, 1985; Parry et al., 1984). These studies have described sericites as being composed of muscovite, phengite, illite, hydromica, or mixed-layer I/S, with fixed interlayer cation contents that usually are less than the structural limit of 1.0 equivalent per $O_{10}(OH)_2$. Sericite has sharp 10 angstrom and integral higher order reflections in XRD analyses. In the Hirshey #2 core samples sericite is identified on the basis of these sharp 10 angstrom and integral higher order reflections, indicating zero, or nearly zero, percent expandability.

The photomicrographs shown in Figures 18c, d, and e show sericite replacing quartz and other clastic grains at

and below the 9049 ft. level in core samples from the Hirshey #2 well. This type of texture was not observed above 9049 feet, and sericite was not observed in XRD patterns from samples above 9049 feet.

XRD analyses of randomly oriented <0.5 micron size fractions from the Hirshey #2 11873 and 11874 foot core samples show that the sericite in these samples is a mixture of 1m and $2m_1$ polytypes. Eberl et al. (1987) found that hydrothermal sericite from the from the Silverton Caldera also consists of a mixture of 1m and $2m_1$ polytypes.

The paragenesis of the sericite and coexisting I/S in these samples is not known. It is possible that the sericite is the end product of the progressive illitization reaction of smectite shown by trends in the cuttings samples, or that it crystallized as a separate phase unrelated to the illitization process. If the sericite does represent the end product of illitization, the coexisting I/S may be the result of a separate nucleation event which formed a separate population of small fundamental particles (Eberl and Srodon, 1988).

The core samples show wide I/S expandability variations over relatively short stratigraphic distances, such as the range from 7889 ft. to 7958 ft. in which <0.5 micron fraction samples vary from 5 to 20 percent expandability (Figure 9). This I/S expandability variation may result from compositional differences of interstitial fluids, controlled by variations in rock fabric and permeability over small stratigraphic distances. They cannot be due to temperature variations because temperatures would not vary significantly over such short stratigraphic distances (Howard, 1986; Boles and Franks, 1979).

Core samples compared to cuttings samples.

I/S expandability and ordering are significantly different in core and cuttings samples from the same stratigraphic horizons (Figures 9 and 10). In addition, sericite and I/S coexist in the core samples below 9049 feet in the Hirshey #2 well, whereas sericite was not detected in any of the cuttings samples from the same depth range.

Drill cuttings samples are collected over a range of depths, and are a mixture of the rock in the depth range. Thus, I/S expandability measurements do not represent the

I/S expandability for any one stratigraphic layer. Instead, they represent an average value for the depth range. Samples taken from narrow stratigraphic horizons within a core represent a specific depth and lithology in a sedimentary section. Mineral assemblages observed from core samples provide a more realistic view of the mineral assemblages forming at a specific stratigraphic horizon than do the mineral assemblages observed from cuttings.

Tarasovite.

The 7958 ft. core sample from the Hirshey #2 well approaches a nearly ideal 3 to 1, I to S ratio and is R3 ordered (Figure 14). This type of I/S has been called "tarasovite" by previous workers (Lazarenko, 1949, 1965; Lazarenko and Korolev, 1970; Brindley and Susuki, 1983). XRD data from this sample show a 47 angstrom reflection and near-integral higher order reflections. Peaks between 10 and 15 degrees two-theta, and several distinctive reflections between 50 and 90 degrees two-theta are particularly diagnostic of a 3:1 I to S ratio and R3 ordering. Figure 13a shows the experimental <0.1 micron XRD pattern for sample 7958 compared with a pattern calculated using the NEWMOD computer program (Reynolds,

1985) for an R3 ordered I/S with 18 percent expandable layers. Figure 13b shows the 47 angstrom reflection from the same sample obtained from a low angle XRD scan using 0.1 degree convergence and divergence slits.

The calculated pattern in Figure 13a was made using a defect broadening parameter with a mean defect-free distance of seven unit cells (unit cell = one 2:1 layer as used in NEWMOD), with a particle thickness distribution that has a low N of two unit cells, and a high N of 21 unit cells (N = number of unit cells in the C direction in a coherent diffraction domain). The calculated pattern for the 50 to 90 degree two-theta range was constructed by calculating two patterns with the same defect broadening parameters, but with different specific wavelength values for Cu K alpha 1 and Cu K alpha 2 radiation. The two patterns were then added together using NEWMOD'S MIXER option (Reynolds, 1985) in a 2:1 ratio for Cu K alpha 1 to Cu K alpha 2. This was done because Cu K alpha 1 radiation is twice as intense as Cu K alpha 2 radiation in this angular range (R.C. Reynolds, personal comm.). The wavelength values used for Cu K alpha 1 and Cu K alpha 2 were 1.5410 and 1.5440 angstroms respectively (Parrish and

Mack, 1963).

The absence of the 87.5 degrees two-theta peak from the experimental pattern could be due to the near perpendicular angle of the incident beam on the sample. If the sample is not infinitely thick with respect to the x-ray beam, the reflection at such a high angle may not be sufficiently intense to be detected.

In a MacEwan crystallite model (Moore and Reynolds, 1989), where I/S is a sequence of interlayers within a single crystallite, I/S with an exact 3:1 I to S ratio would be 25 percent expandable. Brindley and Suzuki (1983) measured expandability in tarasovite at approximately 20 percent smectite layers. Brindley and Suzuki (1983) attributed the lower expandability relative to an exact 3:1 I to S ratio, to the addition of random illite layers in tarasovite MacEwan crystallites.

The tarasovite structure can also be described by a fundamental particle model (Nadeau et al., 1984) in which fundamental illite particles four 2:1 layers thick are arranged in stacks (Figure 19).

The expandability of sample 7958 was measured at 18 percent, lower than the ideal expandability of perfect

tarasovite. In the context of fundamental particle theory the addition of a small number of thicker fundamental particles in a stack dominated by four 2:1 layer particles, could also account for the lower than ideal 25 percent expandability because there would be relatively fewer expandable interfaces in the stack (Figure 20).

NEWMOD calculations show that if all of the fundamental particles were exactly four layers thick, as in perfect tarasovite, the XRD peaks would be very sharp and narrow, more so than in the XRD pattern from Sample 7958. A small proportion of thicker particles as shown in Figure 20 would broaden the peaks to be similar to those of Sample 7958.

The limited peak broadening and the 47 angstrom and higher order reflections in the XRD patterns from Sample 7958 implies that the sample has a limited distribution of sizes of fundamental particles, and a high proportion of four layer illite particles (Figure 20). This interpretation appears inconsistent with an Ostwald Ripening model of clay diagenesis (Eberl and Srodon, 1988), in which smaller crystallites, once formed, dissolve and recrystallize to form larger crystallites, producing a broad distribution of fundamental particle sizes.

Thus if the Ostwald Ripening model is correct, this sample appears to represent a modification or change in the normal process of Ostwald Ripening. The limited particle size distribution and the interruption of Ostwald Ripening suggest stability or metastability of four layer fundamental particles.

Velde et al. (1986) and Jennings and Thompson (1986) have observed that R3 ordering occurs at about 80 percent illite layers in I/S. At that point, the rate of the illitization reaction decreases (e.g. Figure 21). This relationship supports the suggestion that fundamental particles four 2:1 layers thick, with R3 ordering may be metastable or stable.

Further evidence of interparticle diffraction from fundamental particles.

Table 10 shows XRD results from successively smaller size fractions from the Hirshey #2 11000, 10982, and 11874 ft. core samples. Measured expandability of I/S increases in successively smaller size cuts. A higher population of smaller fundamental particles would produce a higher percentage of expanding interfaces when particles stack on XRD slide preparations (Nadeau et al., 1984; Eberl et al.,

1987). Therefore, the fact that successively smaller size fractions show successively higher expandabilities appears to support a fundamental particle interpretation of these mixed-layer I/S clays.

The smallest size fraction analyzed from the 11000 ft. sample, <0.03 microns, was slightly less expandable than the next larger size fraction. This may be due to the thin concentration of the clay suspension used to make the XRD slide. A thin clay concentration would result in shorter stacks of fundamental particles, with fewer expanding interfaces. This observation is similar to those found by Eberl et al., (1987).

Authigenic mineral growth.

Clay textures seen with SEM indicate authigenic crystal growth (Figure 16a, b, c). EDX analysis of these clays indicate that the crystals have a high potassium content and are therefore illite or sericite (Figure 17a, b, c). These data suggest that illite or sericite grew from solution. Authigenic sericite growth is also documented from thin sections (Figure 18).

Figure 16d and 16e show euhedral quartz and K-feldspar, respectively. EDX analyses (Figure 17) show a high silicon

peak and no potassium peak in Figure 17d, and a high potassium peak in Figure 17e. The size and morphology of these crystals, along with feldspar peaks in the <0.1 micron XRD patterns from this stratigraphic interval (e.g. Figure 15), indicate authigenic K-feldspar and quartz growth. The growth of K-feldspar contrasts with data from the Gulf Coast and Colorado River delta where K-feldspar appears to be consumed with increasing depth (Hower et al., 1976; Jennings and Thompson, 1986).

SUMMARY OF CONCLUSIONS.

1) I/S expandability trends seen in cuttings samples in the Tertiary non-marine sediments of southwestern Montana have abrupt discontinuities coincident with stratigraphic unconformities. These discontinuities may result from: a) system composition differences due to differences in sediment types above and below the unconformities, b) compositional differences in interstitial waters resulting from rock fabric variations above and below the unconformities, c) compositional differences resulting from differences in climatic conditions during the deposition of the sediments above and below the unconformities, d) a two-stage burial event with erosion and cooling separating the

two stages, or e) a combination of these models.

2) In the core samples a wide range of I/S expandabilities occurs within a short stratigraphic interval. This variation may be due to differences in rock and fluid compositions, and/or fluid composition differences resulting from rock fabric variations.

3) Sericite coexists with I/S in the deep portions of the Hirshey #2 well. The sericite may represent the end product of progressive illitization of I/S and the I/S may have grown during a separate nucleation event. Alternatively, the sericite may be unrelated to an illitization process and may have nucleated separately.

4) The percent expandability of I/S in a single sample increases in progressively smaller size fractions. This relationship supports the interpretation that the I/S in these samples consists of fundamental particles rather than MacEwan crystallites.

5) Mineral assemblages and diagenetic trends in cuttings samples are significantly different from those observed in core samples. Core samples depict the mineralogy of narrow stratigraphic horizons, in contrast to mineralogic analyses of cuttings samples which represent an average mineralogy

for a relatively broad stratigraphic range.

6) The 7958 ft. core sample contains an R3 ordered I/S with a nearly ideal 3:1 illite to smectite ratio, similar to the mineral tarasovite. The structure of this I/S is consistent with a sample dominated by stacks of four 2:1 layer illite particles with small proportions of thicker particles randomly interstratified among the four-layer particles.

7) A high population of four-layer fundamental particles, viewed in conjunction with an Ostwald Ripening model of clay diagenesis, suggest stability or metastability of fundamental particles four 2:1 layers thick with R3 ordering.

REFERENCES CITED

Beaufort, D., and Meunier, A. (1983) A petrographic study of phyllic alteration superimposed on potassic alteration: The Silbert porphyry deposit (Rhone, France). Economic Geology, 78, 1514-1527.

Boles, J.R., and Franks, S.G. (1979) Clay diagenesis in Wilcox sandstones of southwest Texas: implications of smectite diagenesis on sandstone cementation. Jour. Sed. Petrology, 49, 55-70.

Bonorino, F.G. (1959) Hydrothermal alteration in the Front Range mineral belt, Colorado. Geological Society of America Bulletin, 70, 53-90.

Brindley, G.W., and Suzuki, T. (1982) Tarasovite, a mixed layer illite-smectite which approaches an ordered 3:1 layer ratio. Clay Minerals, 18, 89-94.

Burst, J.F., Jr. (1959) Postdiagenetic clay mineral environmental relationships in the Gulf Coast Eocene: in Swineford, A., ed., Clays and Clay Minerals, Proc. 6th National Conference, Berkeley, California, 1957: New York, Pergamon Press, 327-341.

Carroll, D. (1970) Clay minerals: A guide to their X-ray identification. G.S.A. Spec. Paper 126, 7-12.

Cathelineau, M. (1983) Les mineraux phylliteux dans les gisements hydrothermaux d'uranium. II. Distribution et evolution cristallochimique des illites interstratifies, smectites et chlorites. Bulletine Mineralogie, 106, 553-569.

Dunoyer De Segonzac, G. (1970) The transformation of clay minerals during diagenesis and low-grade metamorphism. Sedimentology, 15, 281-346.

Dutta, P.K. and Suttner, L.J. (1986) Alluvial sandstone composition and paleoclimate, II. Authigenic mineralogy. Jour. Sed. Petrology, 56, 346-358.

Eberl, D.D., and Hower, J. (1976) Kinetics of illite formation. Geological Society of America Bull., 87, 1326-1330.

Eberl, D.D., Srodon, J., and Northrop, H.R. (1986) Potassium fixation in smectite by wetting and drying. In J.A. Davis and K.F. Hayes, Eds., Geochemical processes at mineral surfaces. American Chemical Society Symposium Series, 323, 296-326.

Eberl, D.D., Srodon, J., Lee, M., Nadeau, P.H. and Northrop, H.R. (1987) Sericite from the Silverton caldera, Colorado: correlation among structure, composition, origin, and particle thickness. American Mineralogist, 72, 914-934.

Eberl, D.D. and Srodon, J. (1988) Ostwald ripening and short stacks: Application of the Warren-Averbach method to study of fundamental illite particles. American Mineralogist, 73, 1335-1345.

Ehinger, R.F., Goers, J.W., Hall, M.L., Harris, W.L., Illich, H.A., Petkewich, R.M., Pevear, D.R., Stuart, C.J., Thompson, G.R. (1965) Clay mineralogy of Mezozoic sediments in the vicinity of Drummond, Montana. Billings Geological Society 16th Annual Field Conference August 12-14, 1965, Geology of the Flint Creek Range Montana, 58-66.

Fields, R.W., Rasmussen, D.L., Tabrum, A.R., and Nichols, R. (1985) Cenozoic rocks of the intermontaine basins of western Montana and eastern Idaho. S.E.P.M., Cenozoic Paleogeography of West-Central United States Guidebook, 9-36.

Hanson, W.B. (1983) Unpublished report and cross section. Amoco Production Company, Denver, Colorado.

Hendry, D.A.F. (1981) Chlorites, phengites, and siderites from the Prince Lyell ore deposit, Tasmania, and the origin of the deposit. Economic Geology, 76, 285-303.

Horton, D.G. (1983) Argillic alteration associated with the Amethyst vein system, Creede mining district, Colorado, Ph.D. thesis, University of Illinois, Urbana, Illinois.

Horton, D.G. (1985) Mixed-layer illite/smectite as a paleotemperature indicator in the Amethyst vein system, Creede district, Colorado, USA. Contributions to Mineralogy and Petrology, 91, 171-179.

Howard, J.J. (1987) Influence of shale fabric on illite/smectite diagenesis in the Oligocene Frio Formation, south Texas. in Proceedings of the International Clay Conference, 1985, (Schultz, Leonard G., editor et al.), 8, 144-150. Meeting: July 28-August 2, 1985, Denver, CO.

Hower, J., Eslinger, E.V., Hower, M.E., and Perry, E.A. (1976) Mechanism of burial metamorphism of argillaceous sediment, mineralogical and chemical evidence. Geological Society of America Bull., 87, 725-737.

Huang, W.L. (1988) Controls on ordering of mixed-layer smectite/illite: an experimental study. Abstracts and Program, Clay Minerals Society 25th Annual Meeting, September 18-21 Grand Rapids, Michigan.

Iagmin, P.J. (1972) Tertiary volcanic rocks south of Anaconda, Montana. Masters Thesis University of Montana, Missoula, Montana.

Jennings, S., and Thompson, G.R. (1986) Diagenesis of Plio-Pleistocene sediments of the Colorado River Delta, southern California. Journal of Sedimentary Petrology, 56, 89-98.

Kuenzi, W.D., and Fields, R.W. (1971) Tertiary stratigraphy, structure, and geologic history, Jefferson Basin, Montana. Geological Society of America Bull., 82, 3373-3394.

Lazarenko, E.K. (1949) Hydromicas of clay formations. Mineral. Sbornik L'vov Geol. Obshch.3.

Lazarenko, E.K. (1965) A mica-like mineral from Nagolnyi Tarasovki, Donbass. Mineral. Sbornik L'vov Univ. 19.

Lazarenko, E.K., and Korolev, Yu. M. (1970) Tarasovite, a new dioctahedral ordered interlayered mineral. Zapiski Vses. Obshch. 99, 214-224.\ Min. Abstr. 22 (1971) Abstr. 71-2339.\

Le Bel, L. (1979) Micas magmatiques et hydrothermaux dans l'environnement du porphyre cuprifere de Cerro Verde-Santa Rosa, Perou. Bulletin de Mineralogie, 102, 35-41.

McLeod, P.J. (1987) The depositional history of the Deer Lodge Basin, western Montana. Masters Thesis University of Montana, Missoula, Montana.

Meunier, A., and Velde, B. (1982) Phengitization, sericitization and potassium-beidellite in a hydrothermally-altered granite. Clay Minerals, 17, 285-299.

Moore, D.M., and Reynolds, R.C. Jr. (1989) X-ray Diffraction and the Identification and Analysis of Clay Minerals. Oxford New York, Oxford University Press.

Nadeau, P.H., Wilson, M.J., McHardy, W.J., and Tait, J.M. (1984a) Interparticle diffraction: A new concept for interstratified clays. Clay Minerals, 19, 757-769.

Nadeau, P.H., Wilson, M.J., McHardy, W.J., and Tait, J.M. (1984b) Interstratified clays as fundamental particles. Science, 225, 923-925.

Nicot, E. (1981) Les phyllosilicates des terrains precambriens du Nord-Quest du Montana (U.S.A.) dans la transition anchizone-epizone. Bulletin de Mineralogie, 104, 615-624.

Omelyanenko, B.T., Volovikova, I.M., Drits, V.A., Zvyagin, B.B. Andreev, O. V., and Sakharov, B.A. (1982) On the content of sericite notion. Izvestiya Akademii Nauk SSSR, Seriya Geologicheskaya no. 5, 69-86.

Parrish, W., and Mack, M. (1963) Data for X-ray analysis, second edition volume I, charts for solution of Bragg's equation (d versus theta and two-theta for copper K radiation). Philips Labratories, N.V. Philips' Gloeilampenfabrieken, Eindhoven, The Netherlands.

Parry, W.T., Ballantyne, J.M., and Jacobs, D.C. (1984) Geochemistry of hydrothermal sericite from Roosevelt Hot Springs and the Tintic and Santa Rita porphyry copper systems. Economic Geology, 79. 72-86.

Pollastro, R.M. (1982) A recommended procedure for the preparation of oriented clay-mineral specimens for X-ray diffraction analysis: modifications to Drever's filter-membrane-peel technique. U.S. Geol. Surv. Open File Rept. 82-71.

Reynolds, R.C., and Hower, J. (1970) The nature of interlayering in mixed-layer illite-montmorillonites. Clays and Clay Minerals, 18, 25-36.

Reynolds, R.C. (1985) NEWMOD comuter program for the calculation of the one-dimensional X-ray diffraction patterns of mixed-layer clays. R.C. Reynolds, Dept. of Earth Sciences, Dartmouth College, Hanover, NH 03755.

Robinson, R.C. (1967) Geologic map of the Toston quadrangle, southwestern Montana. U.S. Geol. Survey Misc. Geol. Invest. Map I-486.

Shirozu, H., and Higashi, S. (1972) X-ray examination of sericite minerals associated with the Kuroko deposits. Clay Science, 4, 137-142.

Srodon, J. (1980) Precise identification of illite/smectite interstratifications by X-ray powder diffraction. Clays and Clay Minerals, 32, 3337-349.

Srodon, J. (1981) X-ray identification of randomly interstratified illite-smectite in mixtures with discrete illite. Clay Minerals, 16, 297-304.

Srodon, J., (1984) X-ray identification of illitic materials. Clays and Clay Minerals, 32, 337-349.

Srodon, J., and Eberl, D.D. (1984) Illite. Mineralogical Society of America Reviews in Mineralogy, 495-544.

Thompson, G.R., Fields, R.W., and Alt, D. (1982) Land-based evidence for Tertiary climatic variations: Northern Rockies. Geology, 10, 413-417.

Velde, B., Suzuki, T., and Nicot E. (1986) Pressure-temperature composition of illite/smectite mixed-layer minerals: Niger Delta mudstones and other examples. Clays and Clay Minerals, 34, 435-441.

Whitney, G., and Northrop, H.R. (1988) Experimental investigation of the smectite to illite reaction: dual reaction mechanisms and oxygen-isotope systematics. American Mineralogist, 73, 77-90.

APPENDIX - well locations

Deer Lodge Valley

Well name: Benson
Location: SE, SW, Sec. 34, T. 7 N., R. 9 W.
Dates: 7-31-84 to 9-4-84

Well name: Arco
Location: NW, SW, Sec. 3, T. 5 N., R. 10 W.
Dates: 9-30-84 to 11-15-84

Well name: Lewis Johnson
Location: SW, SW, Sec. 31, T. 7 N., R. 9 W.
Dates: 9-19-81 to 5-18-82

Well name: Jacobson
Location: NW, NE, Sec. 25, T. 6 N., R 10 W.
Dates: 3-18-84 to 6-18-84

Well name: Montana State Prison
Location: N, SW, Sec. 2, T. 7 N., R. 10 W.
Dates: 7-5-82 to 8-9-82

Big Hole Valley

Well name: Hirshey #1
Location: NE 1/4, Sec. 27, T. 3 S., R 16 W.
Dates: 1-12-80 to 2-3-81

Well name: Hirshey #2
Location: NW 1/4, Sec. 31, T. 4 S., R 15 W.
Dates: 2-21-83 to 4-22-83

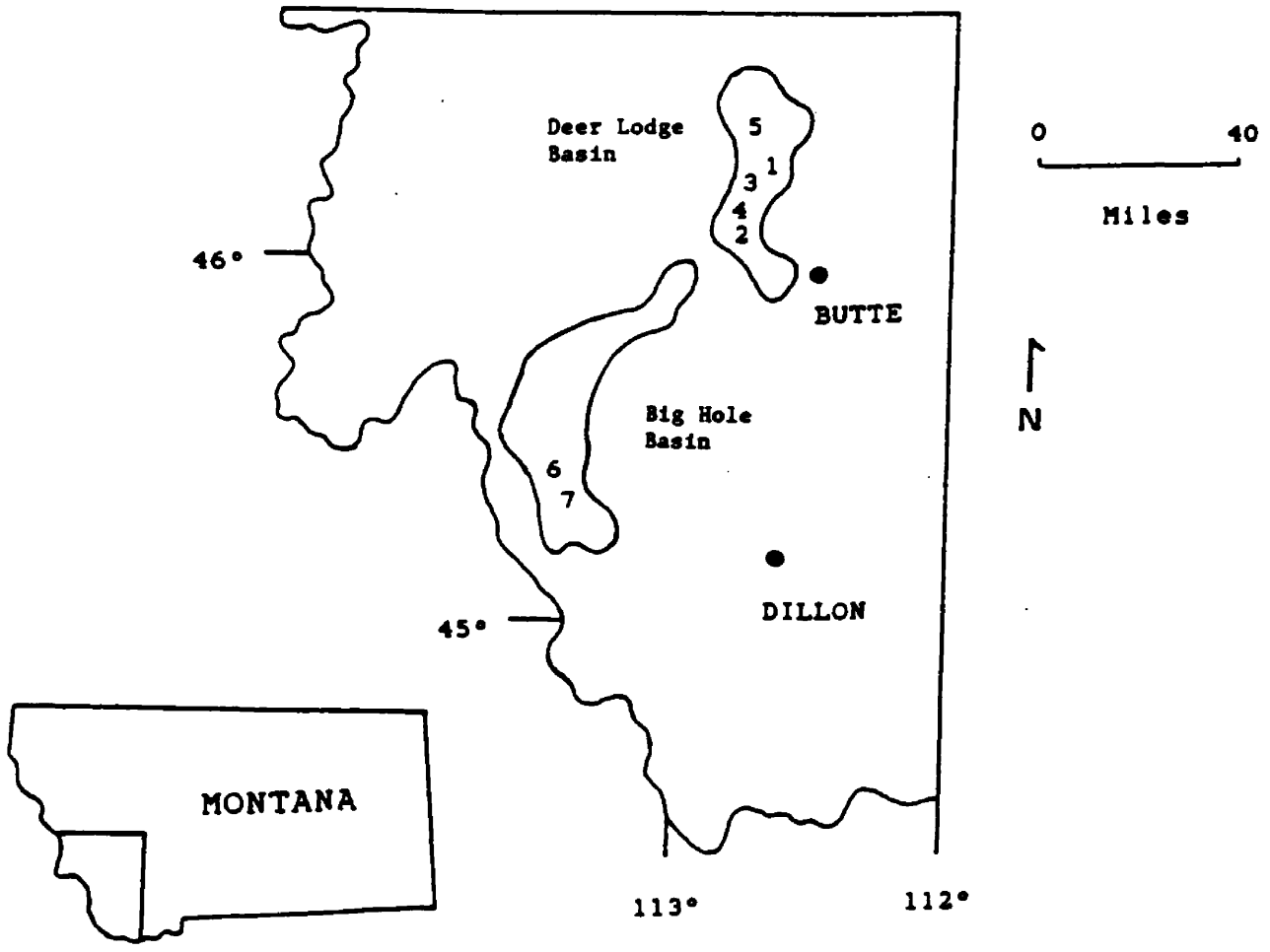

1 = Benson well
2 = Arco well
3 = Lewis Johnson well
4 = Jacobson well
5 = Montana State Prison well
6 = Hirshey #1 well
7 = Hirshey #2 well

Figure 1. Deer Lodge and Big Hole Valleys of southwestern Montana, with relative well locations. See appendix for exact well locations.

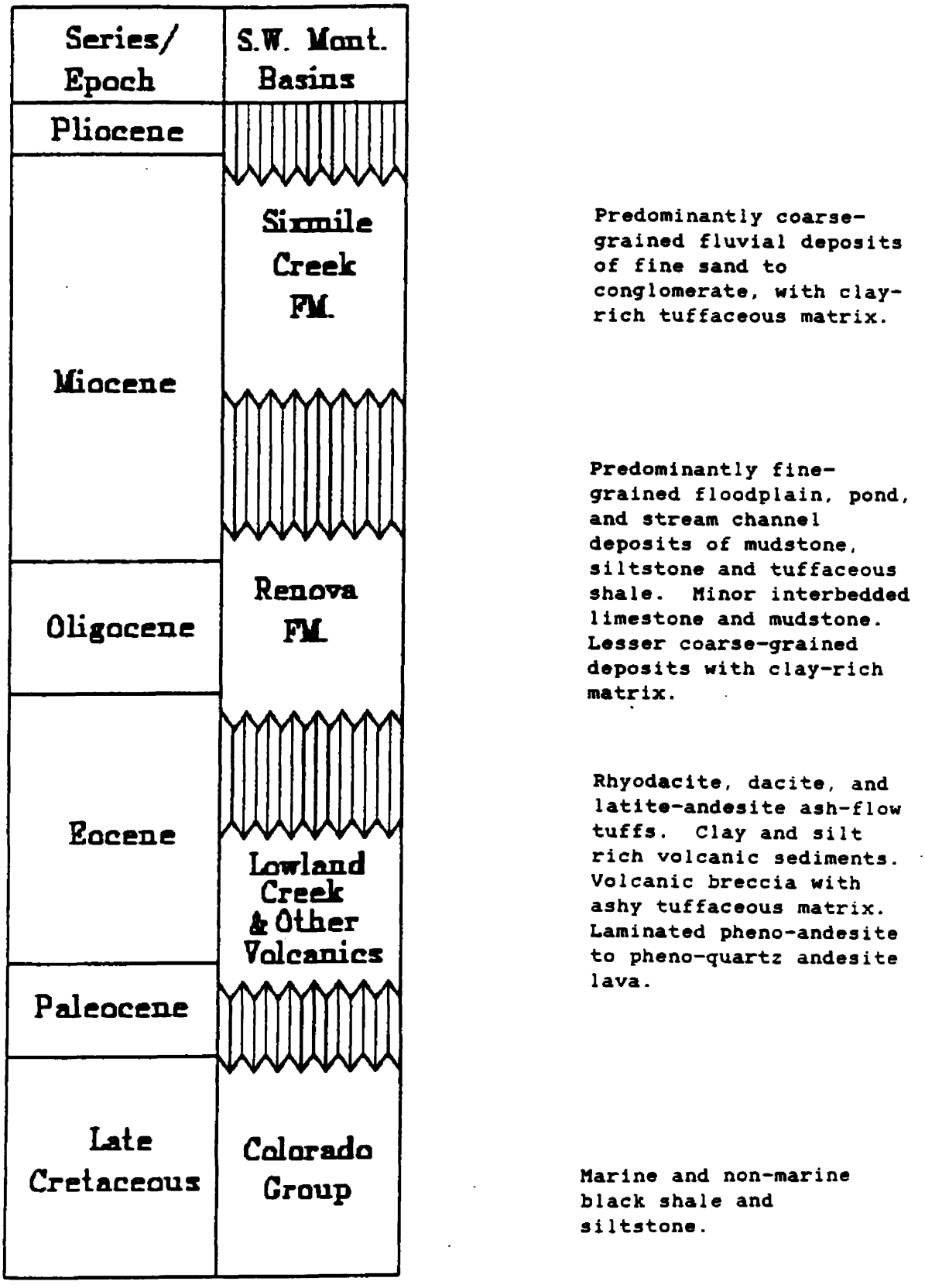

Figure 2. Composite stratigraphy of soutwest Montana basins (Fields et al., 1985; Iagmin, 1972; Ehinger et al., 1965; McLeod, 1987). All units shown are in unconformable contact with adjacent units.

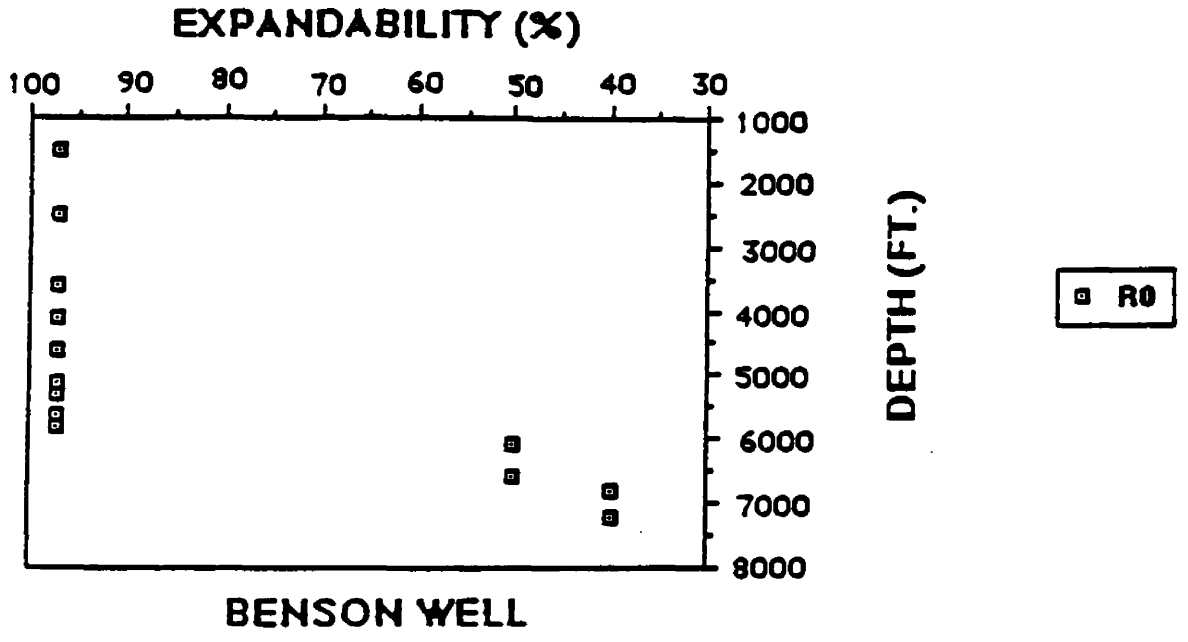

Figure 3. Percent expandability and ordering of illite/smectite compared with depth for the less than 0.5 micron size fraction from drill cuttings.

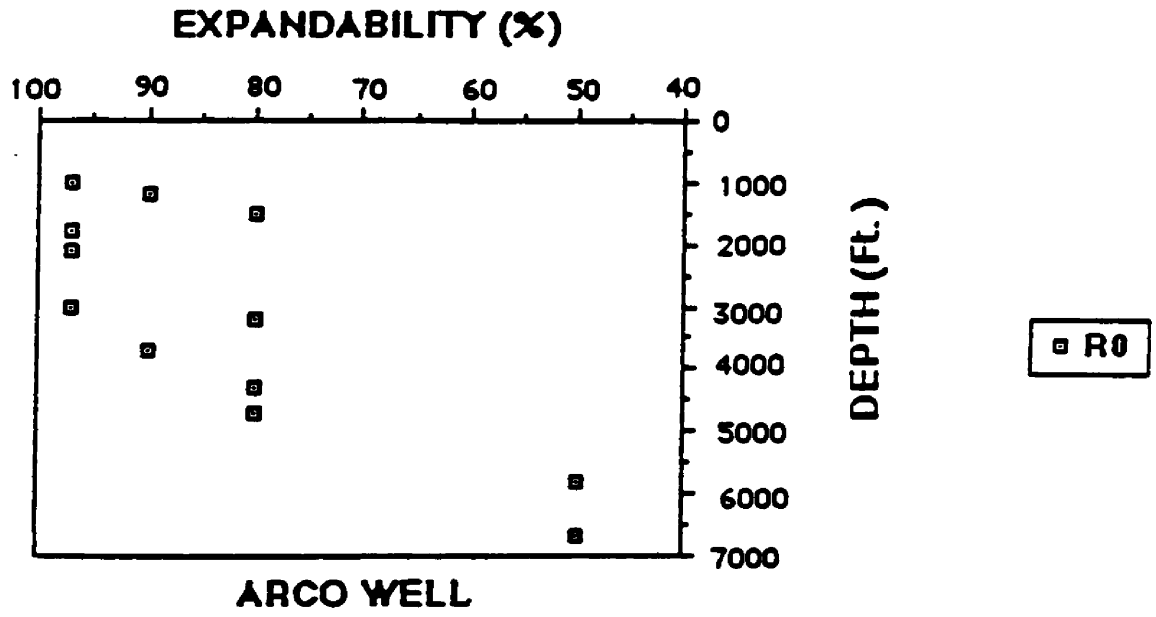

Figure 4. Percent expandability and ordering of illite/smectite compared with depth for the less than 0.5 micron size fraction from drill cuttings.

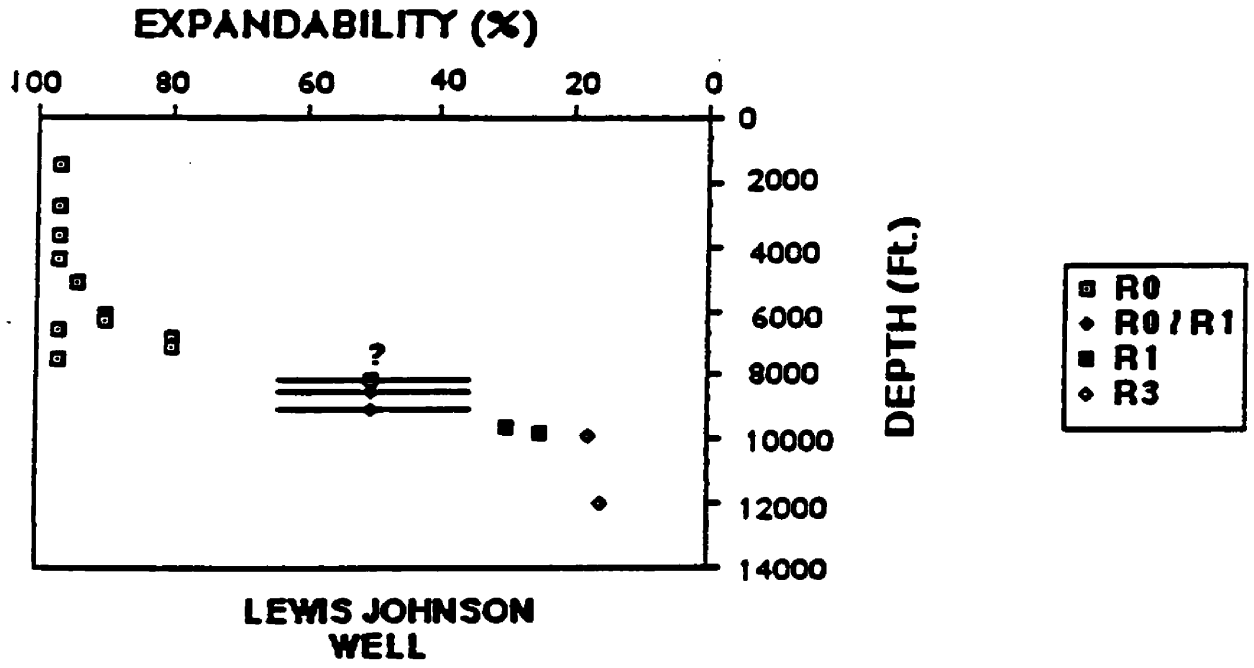

Figure 5. Percent expandability and ordering of illite/smectite compared with depth for the less than 0.5 micron size fraction from drill cuttings. Samples 8000, 8400, and 9000 feet are estimated at 50 percent expandable. Horizontal lines indicate possible ranges of expandabilities.

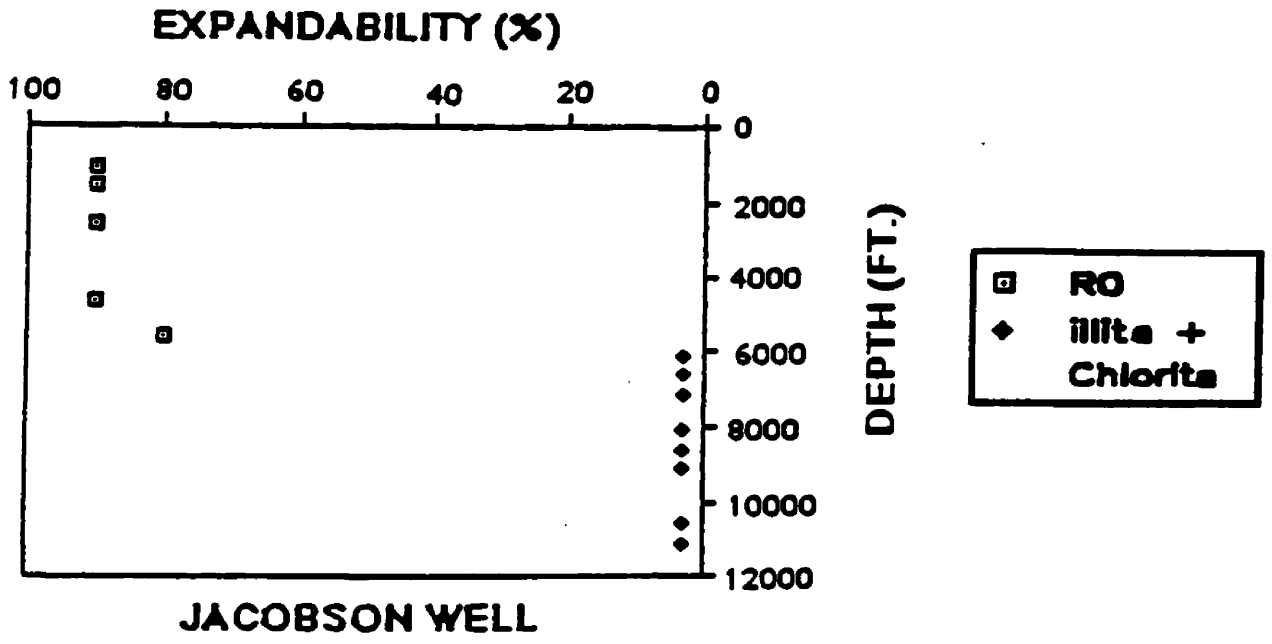

Figure 6. Percent expandability and ordering of illite/smectite compared with depth, and depth of illite + chlorite samples with no measurable expandability. All samples are from the less than 0.5 micron size fraction from drill cuttings.

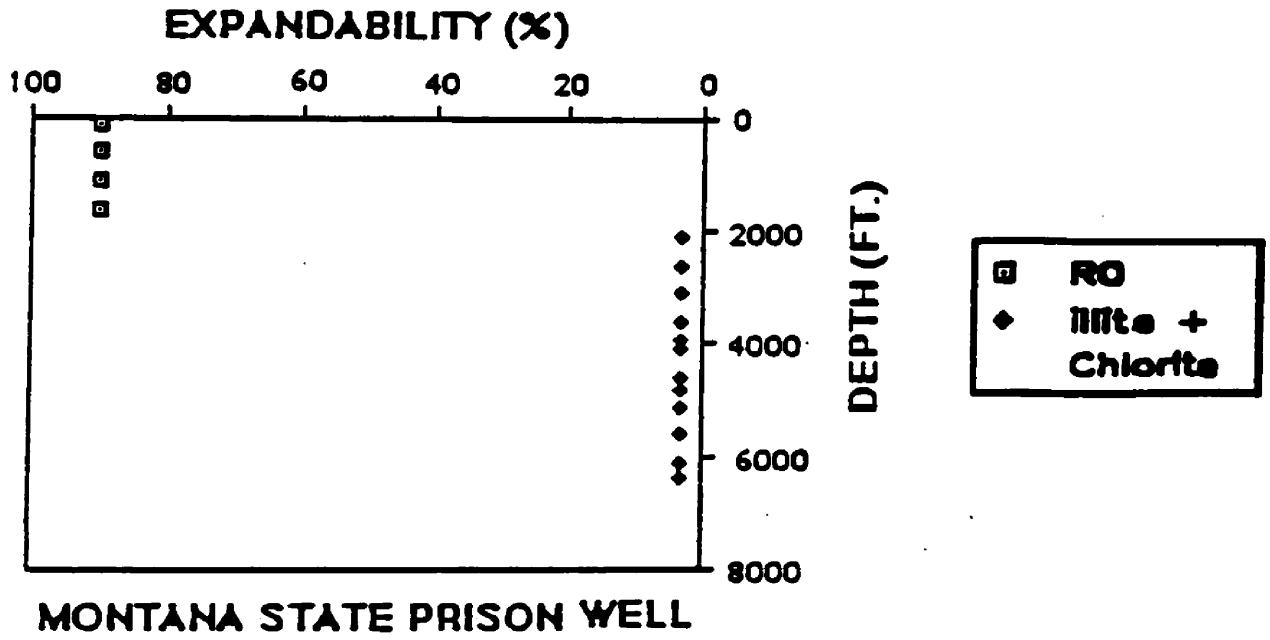

Figure 7. Percent expandability and ordering of illite/smectite compared with depth, and depth of illite + chlorite samples with no measurable expandability. All samples are from the less than 0.5 micron size fraction from drill cuttings.

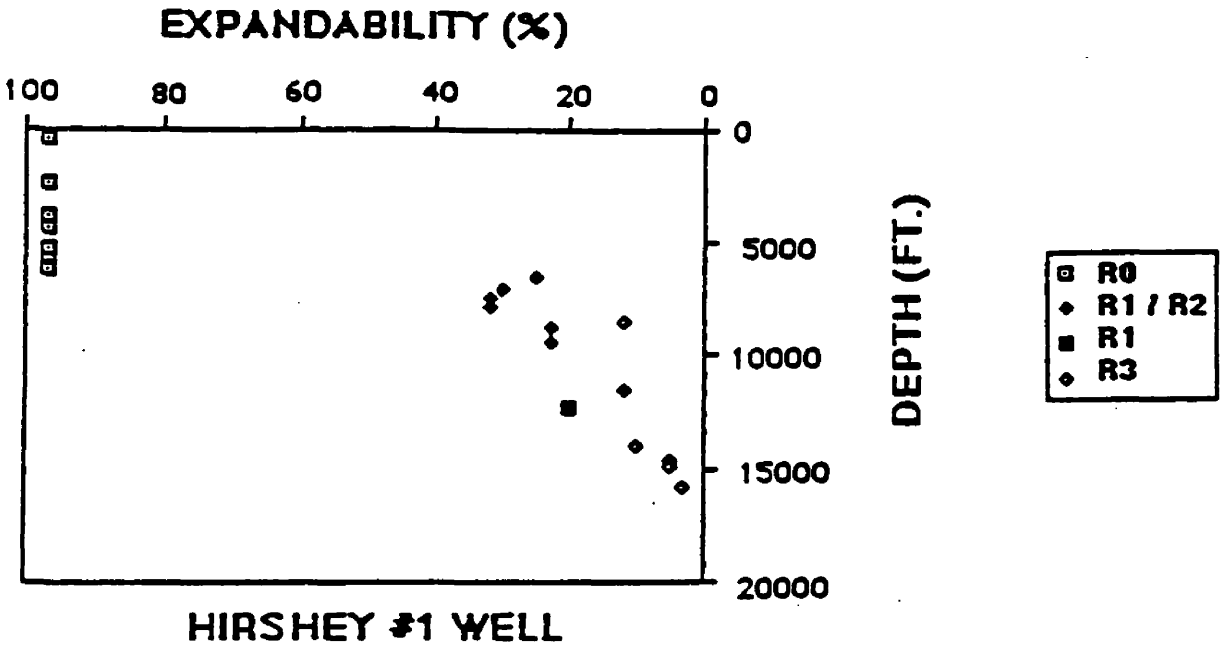

Figure 8. Percent expandability and ordering of illite/smectite compared with depth for the less than 0.5 micron size fraction from drill cuttings.

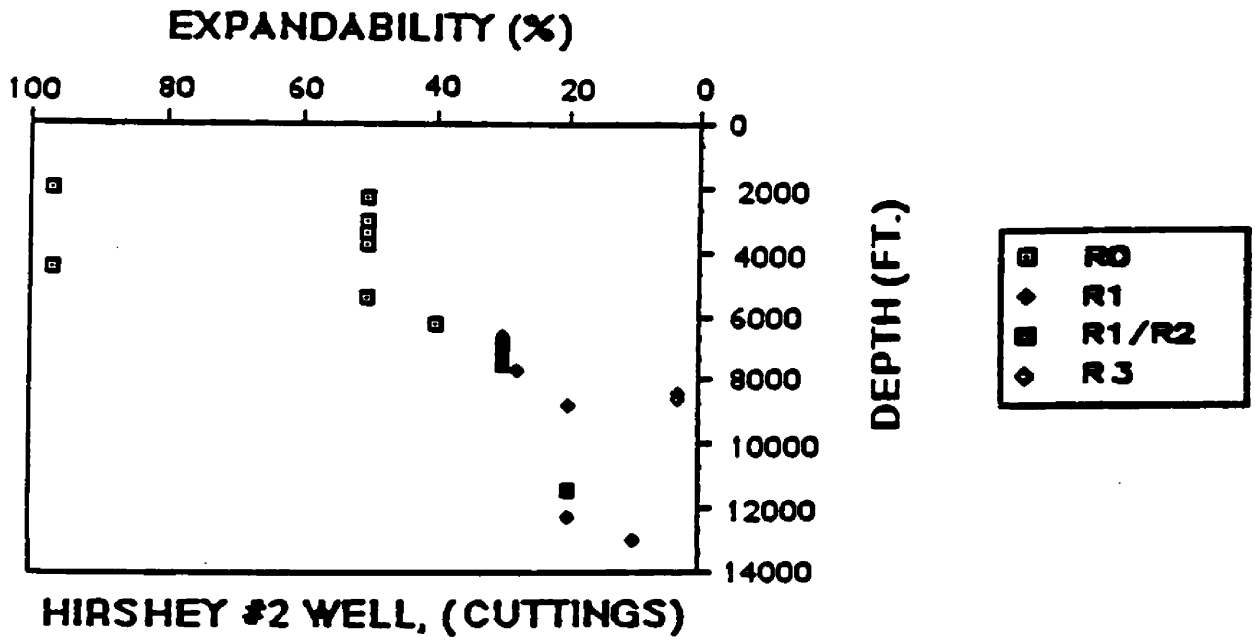

Figure 9. Percent expandability and ordering of illite/smectite compared with depth for the less than 0.5 micron size fraction from drill cuttings.

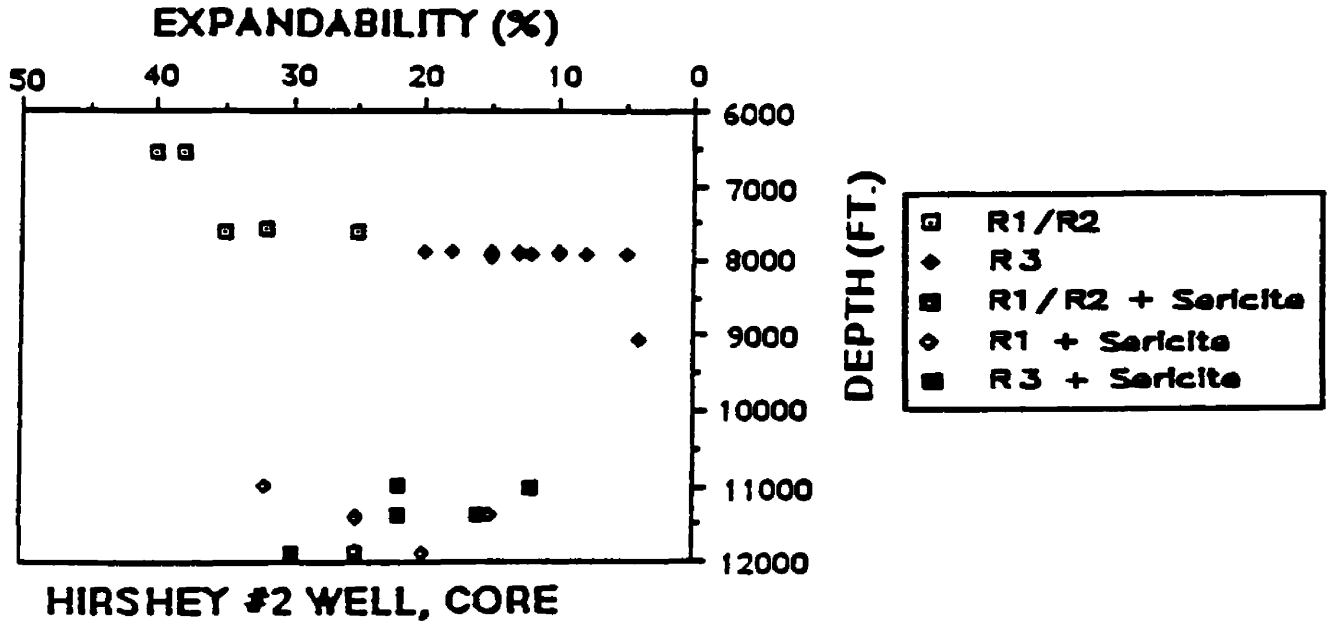

Figure 10. Percent expandability and ordering of illite/smectite (I/S) compared with depth for the less than 0.5 micron size fraction from drill core samples. In all samples at and below 10982 ft. I/S coexists with sericite. Sericite is not plotted separately on the figure.

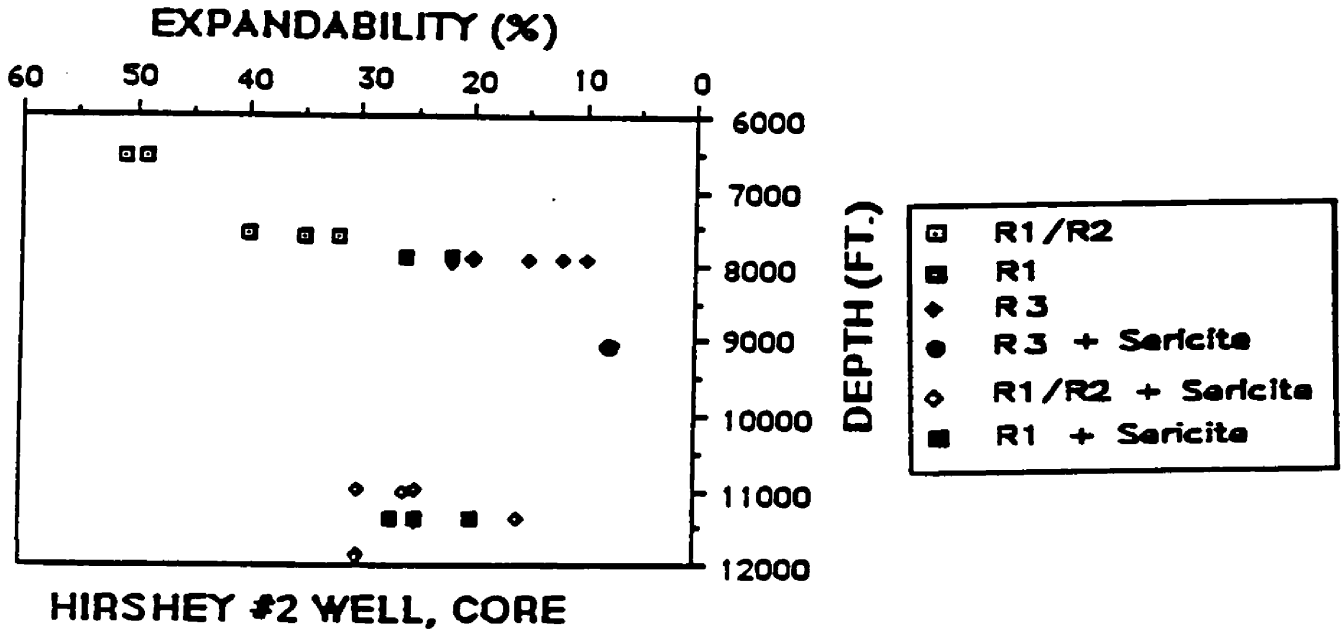

Figure 11. Percent expandability and ordering of illite/smectite (I/S) compared with depth for the less than 0.1 micron size fraction from drill core samples. In all samples at and below 9049 ft. I/S coexists with sericite. Sericite is not plotted separately on the figure.

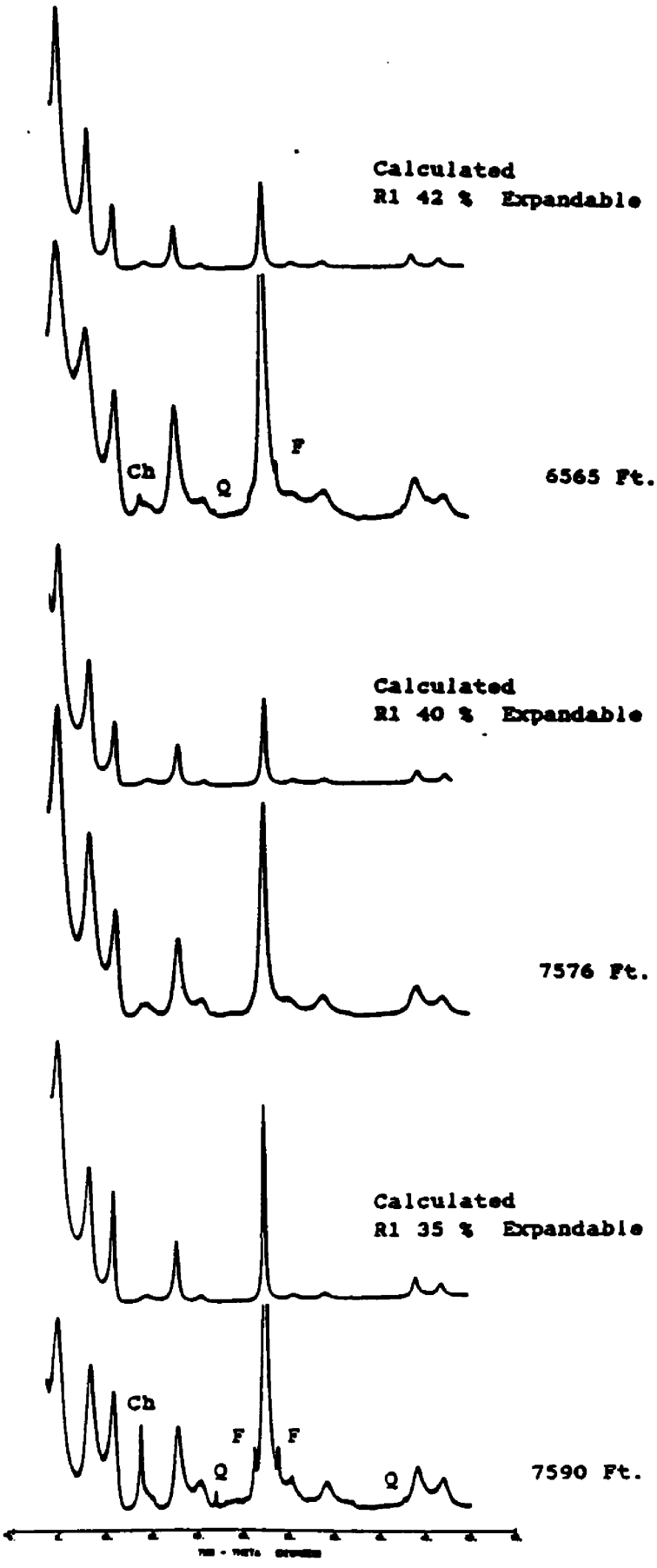

Figure 12.

Measured XRD patterns from the Hirshey #2 6565, 7576, and 7590 ft. core samples compared with calculated illite/smectite (I/S) patterns from NEWMOD (Reynolds, 1985). All measured patterns are from the less than 0.1 micron size fraction. The R1 42 percent expandable and R1 40 percent expandable I/S patterns were calculated with a mean defect-free distance of six 2:1 layers. The R1 35 percent expandable I/S pattern was calculated with a mean defect-free distance of 10 2:1 layers. The I/S from the three experimental samples are R1/R2 ordered, based on parameters outlined by Srodon (1980, 1984). I/S peaks are not labeled. Ch = chlorite, Q = quartz, F = feldspar.

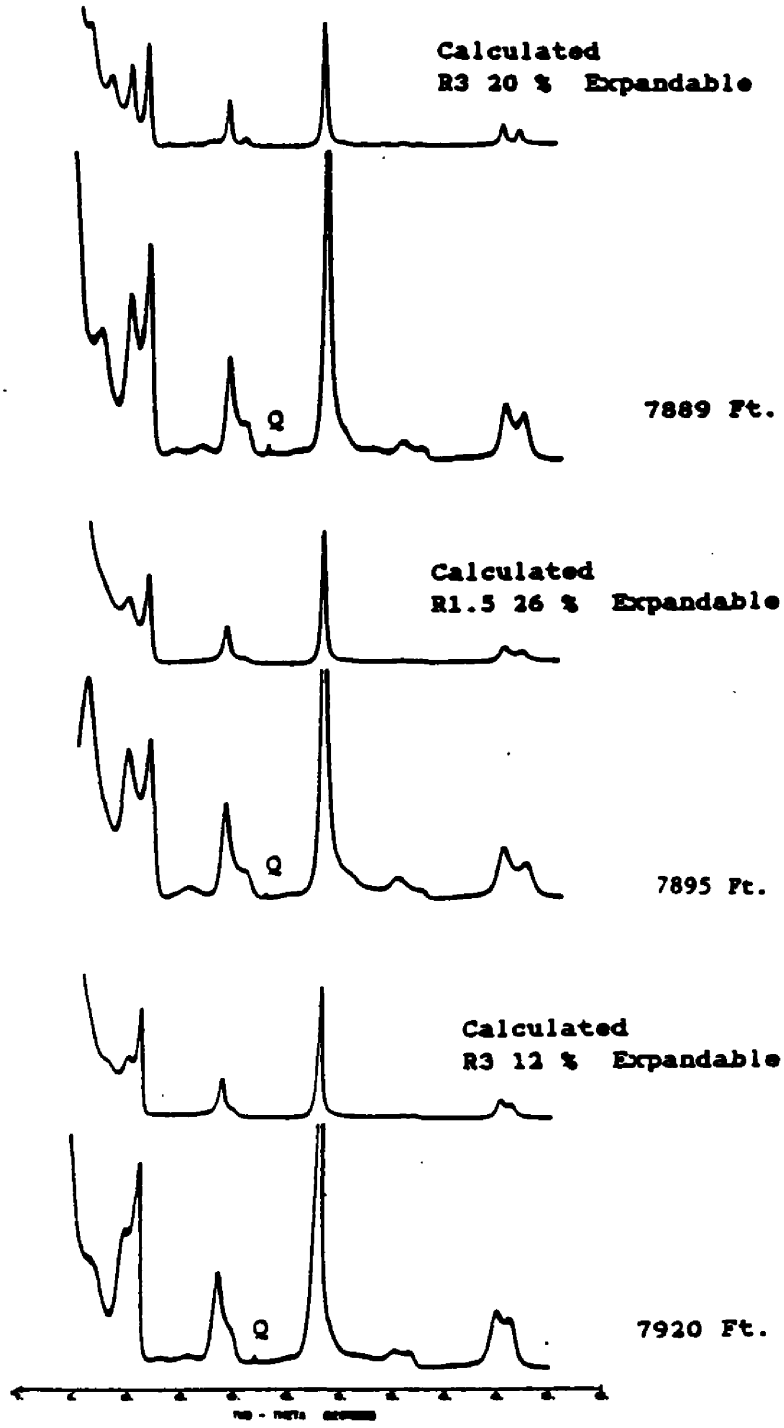

Figure 13.

Measured XRD patterns from the 7889, 7895, and 7920 ft. Hirshey #2 core samples compared with calculated illite/smectite (I/S) patterns from NEWMOD (Reynolds, 1985). All measured patterns are from the less than 0.1 micron size fraction. All NEWMOD patterns were calculated using a mean defect-free distance of eight 2:1 layers. The I/S from the 7889 and 7920 ft. samples are both R3 ordered and the I/S from the 7895 ft. sample is R1/R2 ordered (similar to R1.5 of NEWMOD calculations), based on parameters outlined by Srodon (1980, 1984). I/S peaks are not labeled. Q = quartz.

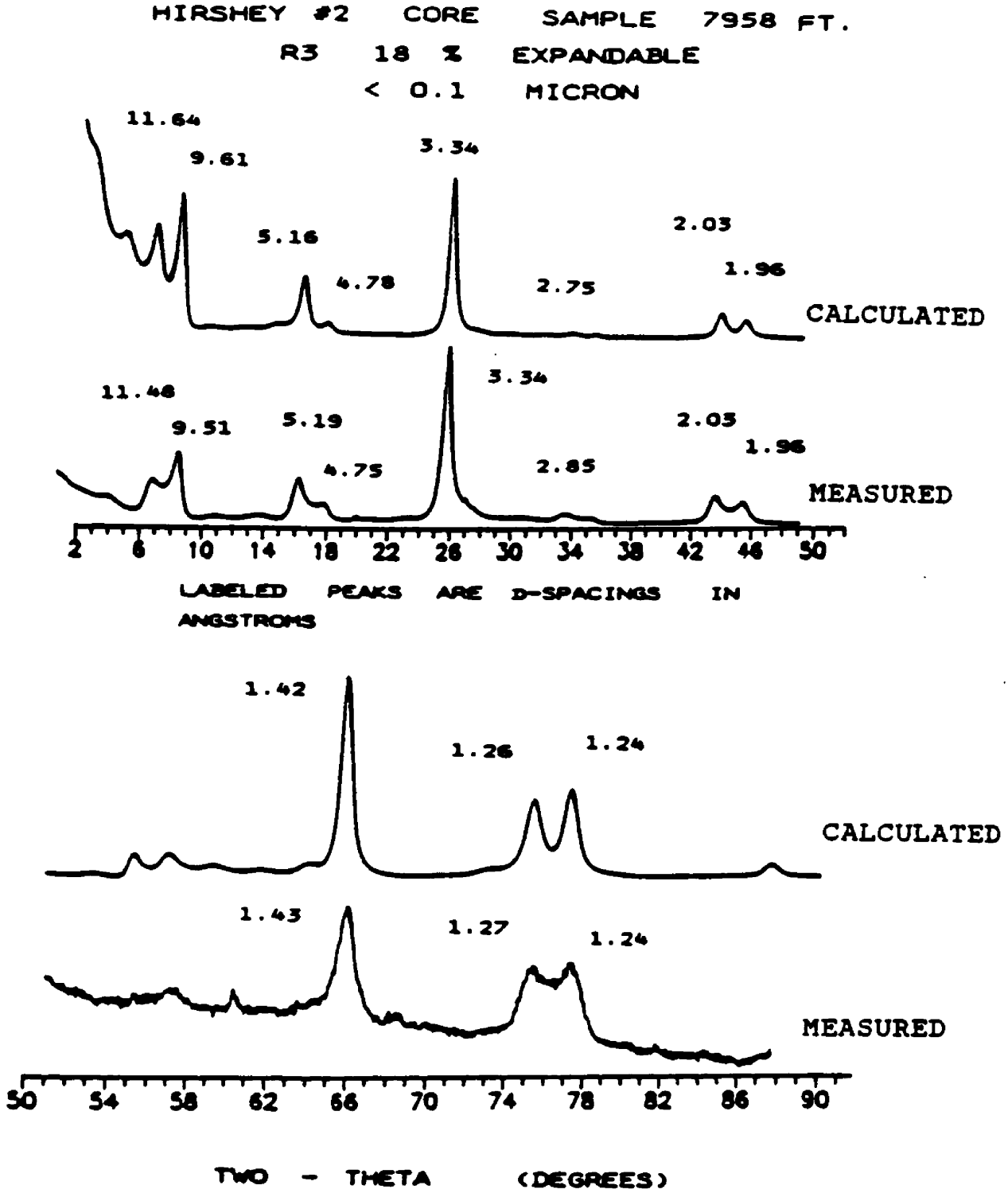

Figure 14a. Measured XRD pattern for the Hirshey #2 7958 ft. core sample from the less than 0.1 micron size fraction, compared with a NEWMOD (Reynolds, 1985) calculated pattern for an R3 ordered 18 percent expandable illite/smectite. The NEWMOD pattern was calculated using a mean defect-free distance of seven 2:1 layers. See Tarasovite section page 25 in text for details on the calculated pattern parameters.

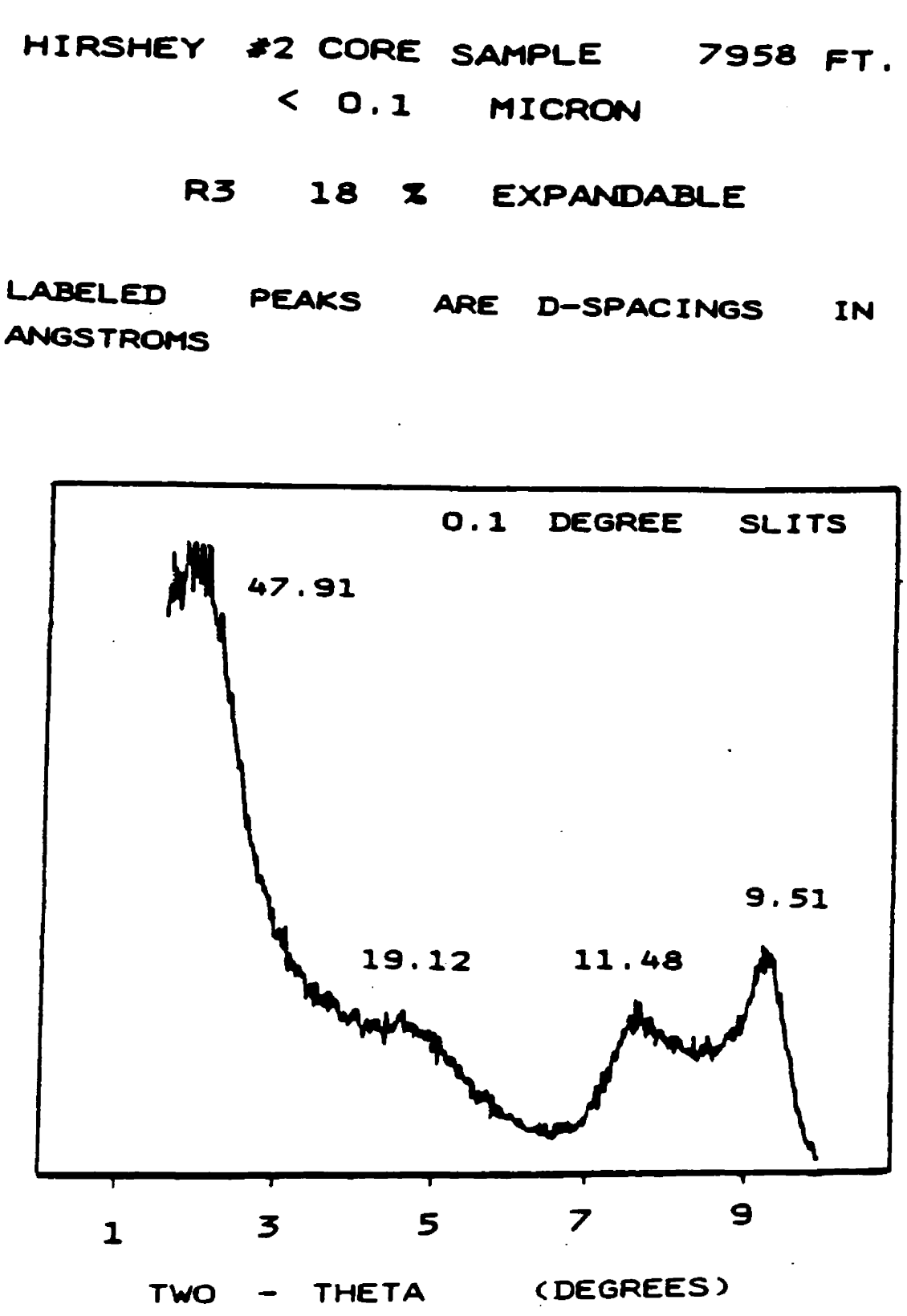

Figure 14b. Low angle XRD pattern ran with 0.1 degree slits, for the Hirshey #2 7958 ft. core sample from the less than 0.1 micron size fraction.

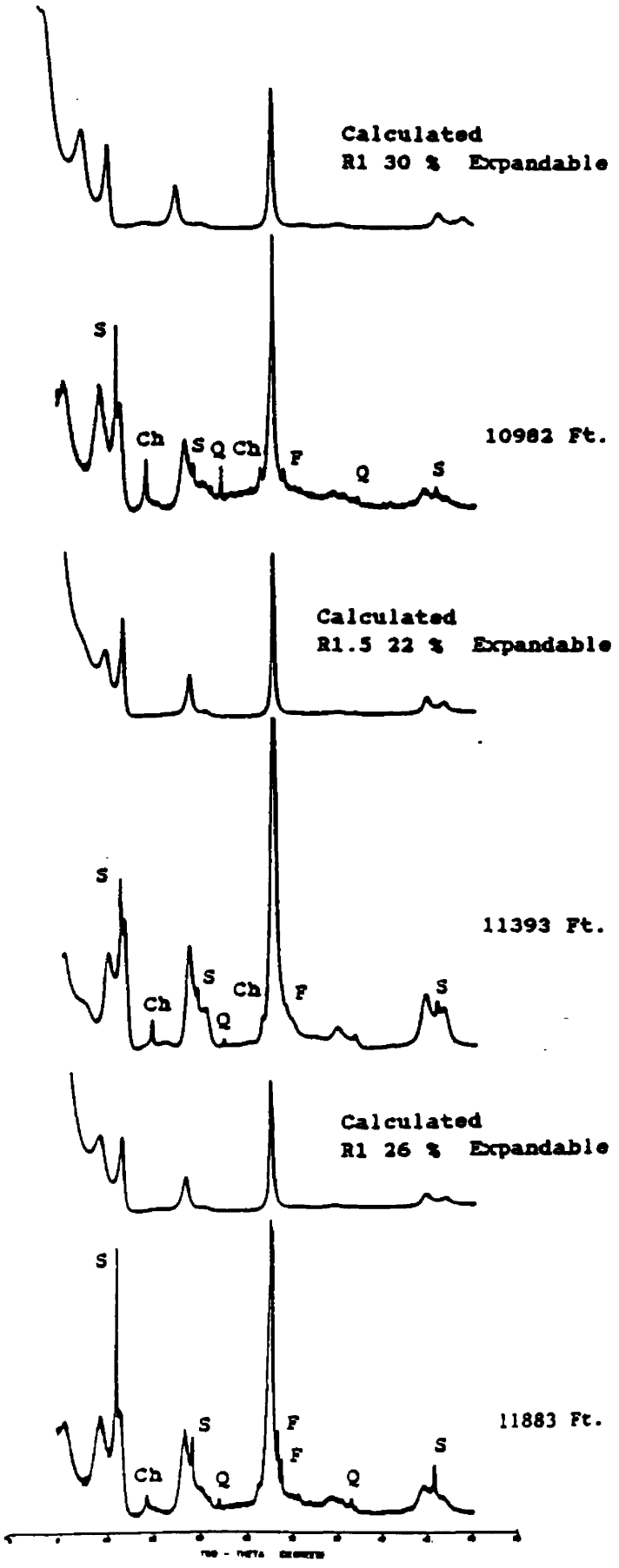

Figure 15.

Measured XRD patterns from the Hirshey #2 10982, 11393, and 11883 ft. core samples compared with calculated illite/smectite (I/S) patterns from NEWMOD (Reynolds, 1985). All measured patterns are from the less than 0.1 micron size fraction. The NEWMOD patterns for the R1 30 percent expandable and R1 26 percent expandable I/S were calculated using a mean defect-free distance of eight 2:1 layers. The R1.5 22 percent expandable I/S pattern was calculated using a mean defect-free distance of 10 2:1 layers. The experimental patterns show that I/S coexists with sericite. The sericite 001, 002, and 005 peaks are labeled. The I/S phases in the experimental samples are all R1/R2 ordered, based on parameters outlined by Srodon (1980, 1984). I/S peaks are not labeled. Ch = chlorite, Q = quartz, F = feldspar, S = sericite.

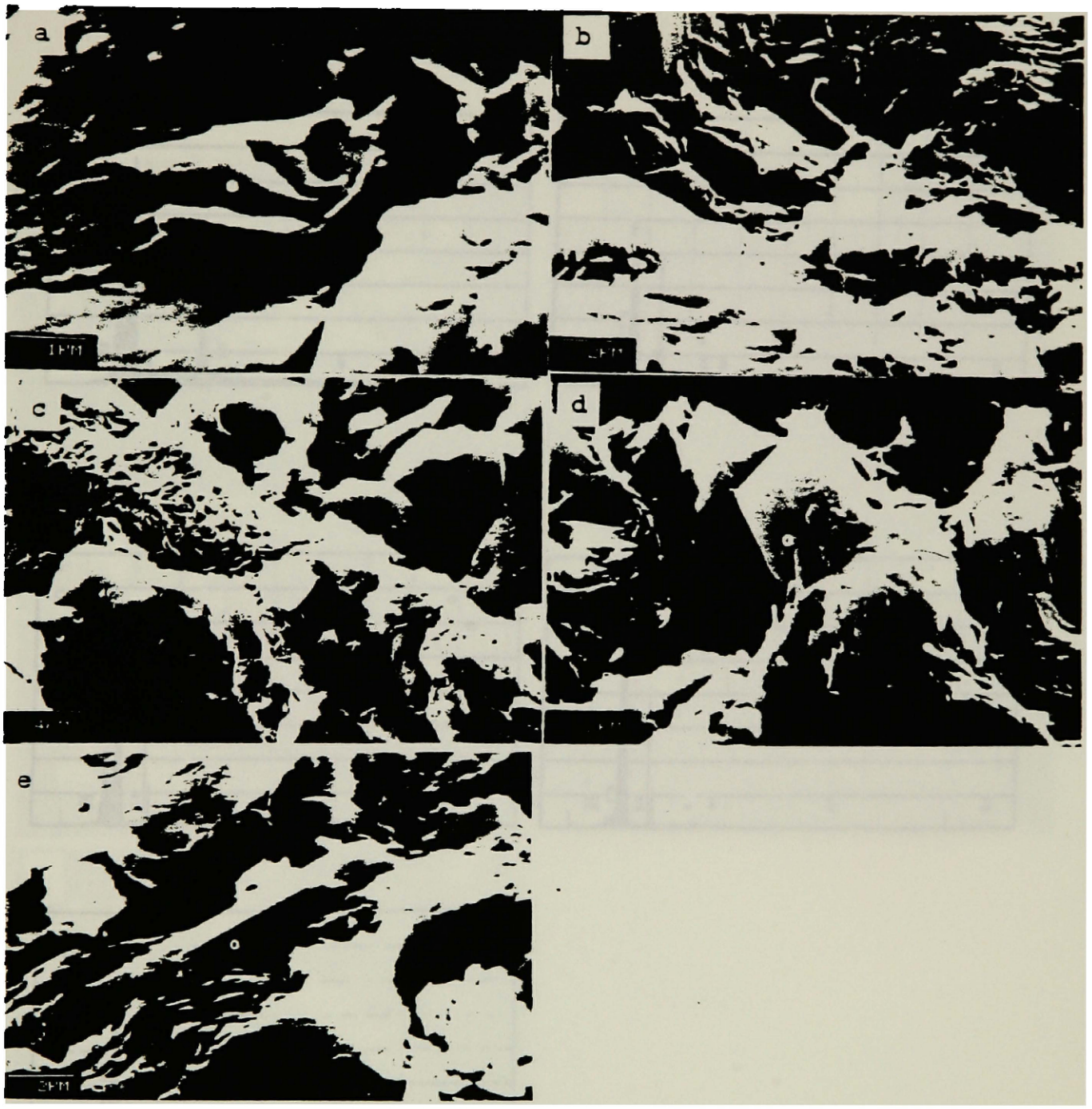

Figure 16. Scanning electron micrographs showing authigenic mineral textures from Hirshey #2 core samples. Figure 15a is from 10982 ft.; 15b, c, and d are from 7902 ft.; 15e is from 11393 ft.. The spot in the center of each photo is the location of the energy-dispersive X-ray analysis (figure 17).

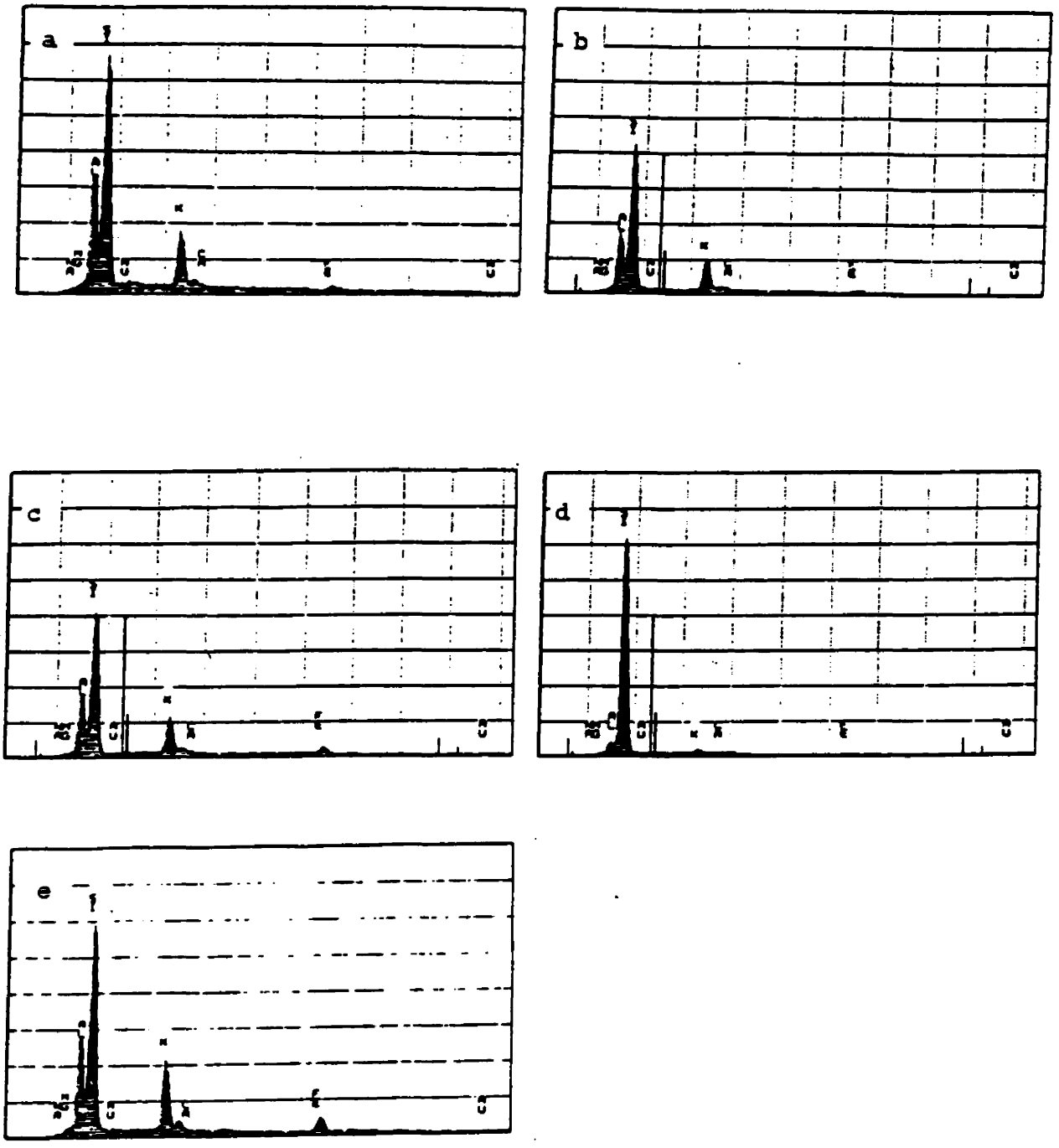

Figure 17. Energy-dispersive X-ray analyses (EDX) corresponding to scanning electron micrographs in figure 16.

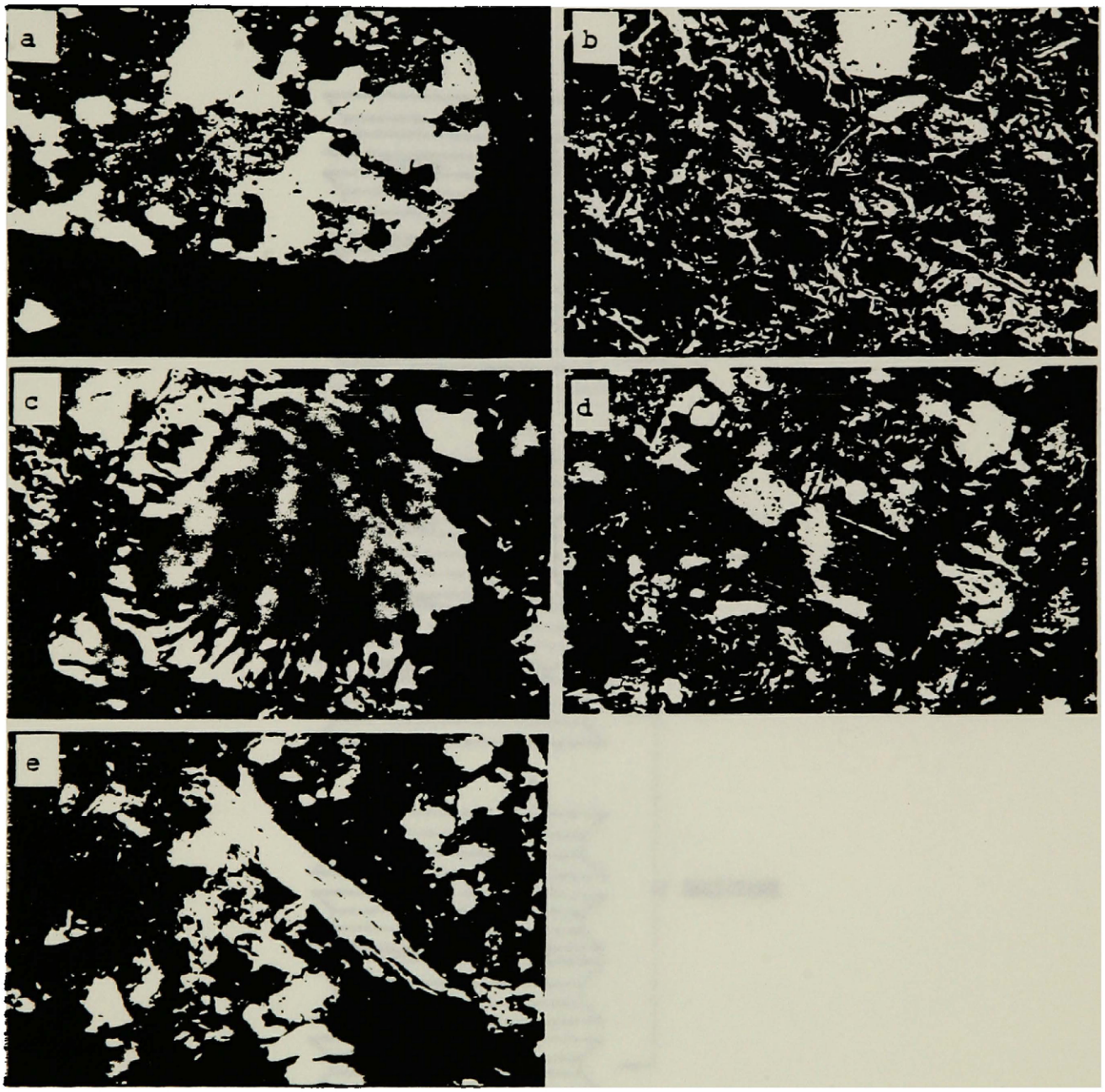

Figure 18. Cross polar photomicrographs showing typical rock fabric and replacement textures from Hirshey #2 core samples. Figure 17a is from 6565 ft.; 17b is from 7890 ft.; 17c, d, and e, are from 11363 ft.

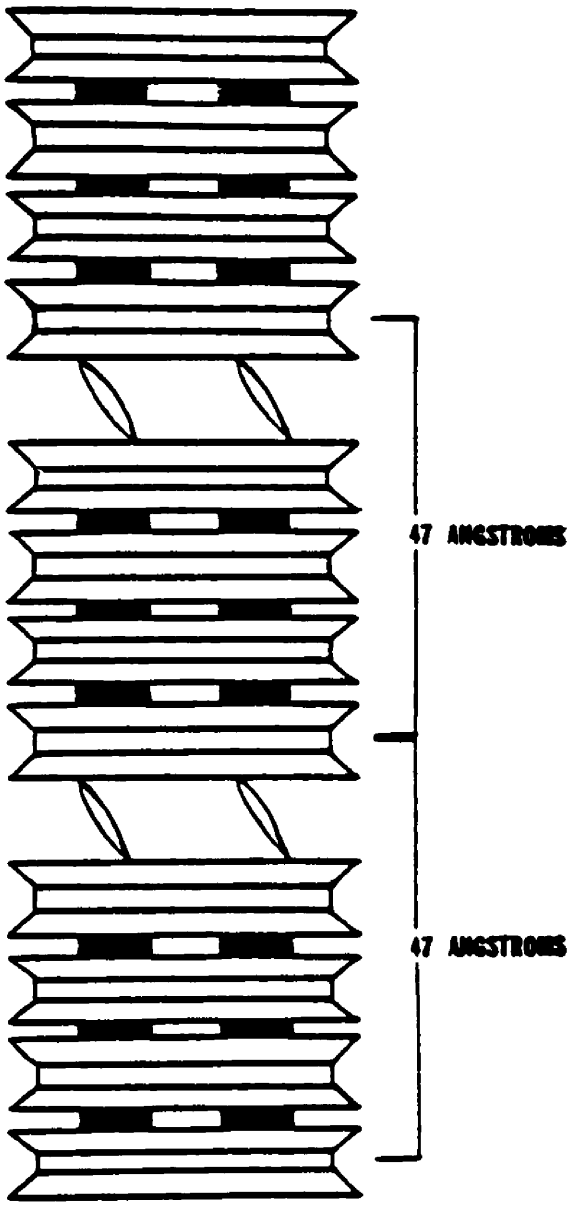

Figure 19. Illustration of a stack of four 2:1 layer fundamental particles expanded with ethylene glycol.

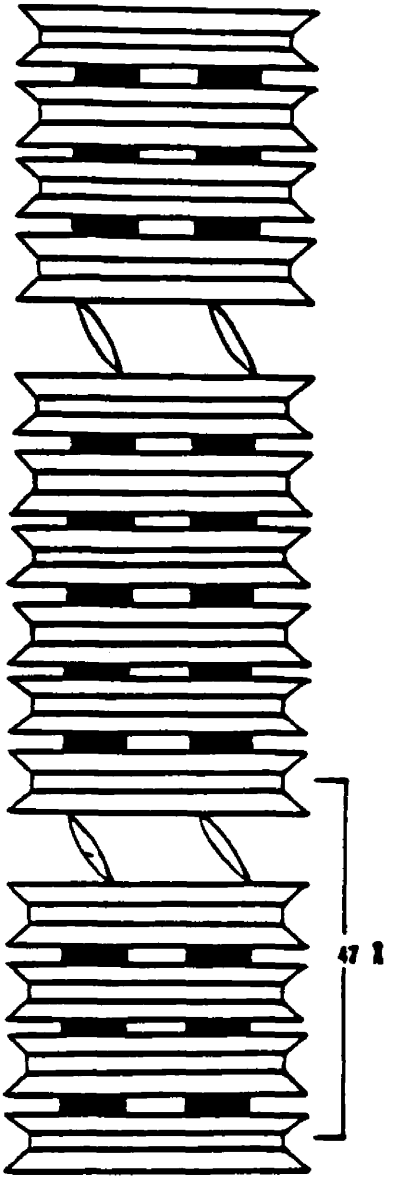

Figure 20. Illustration of four 2:1 layer fundamental particles, in a stack with a thicker fundamental particle expanded with ethylene glycol.

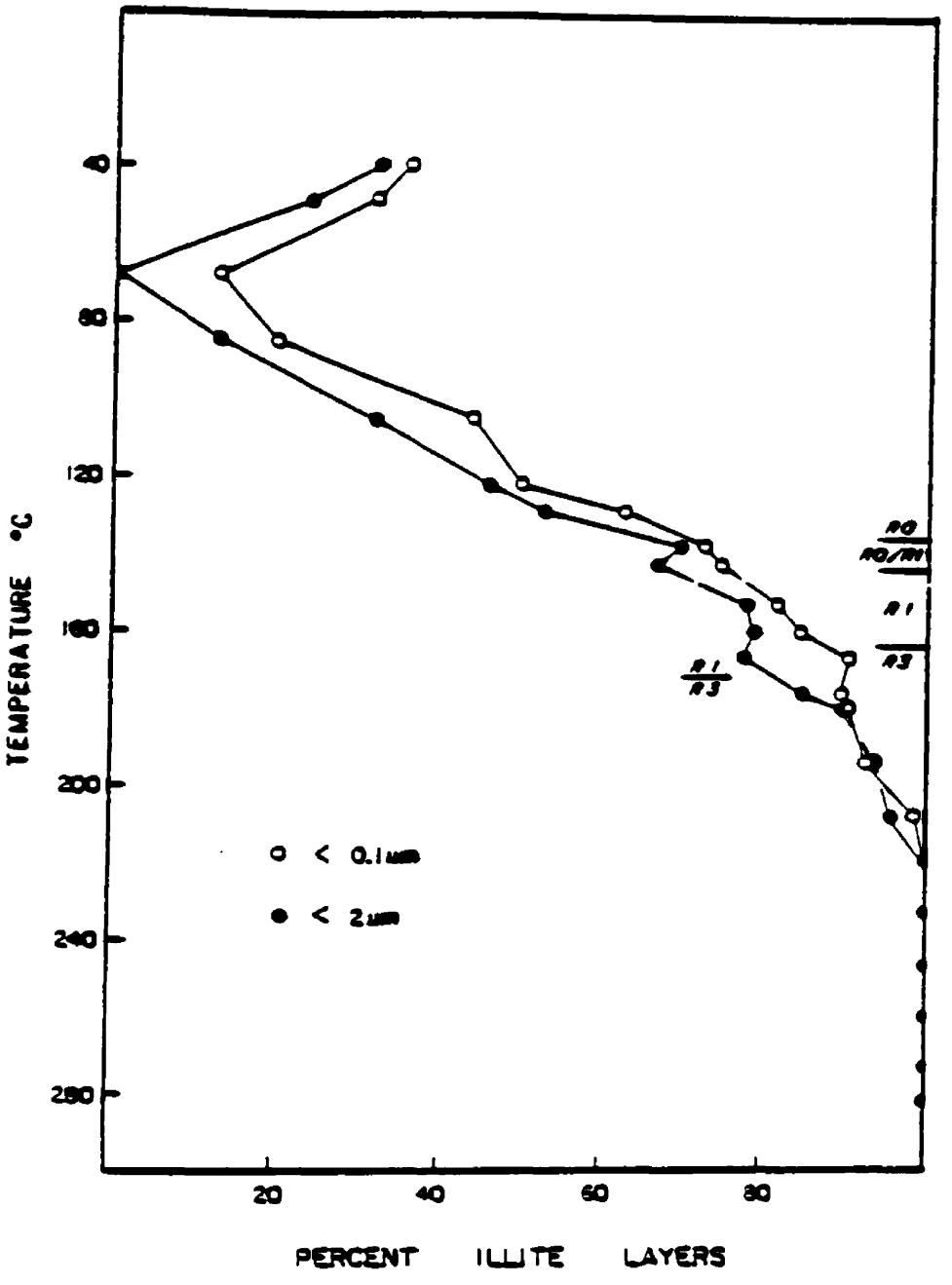

Figure 21. Percentage of illite layers in mixed-layer illite/smectite compared to logged well temperatures, from the Borchard A-2 well Colorado River Delta (from Jennings and Thompson, 1986). Note inflection in curve at transition to R=3 ordering.

TABLE 1. BENSON WELL

Sample	I/S ordering	% Expandability	Accessory Minerals
1500	R0	100	- - -
2500	R0	100	- - -
3600	R0	100	- - -
4000	R0	100	Ch/K
4500	R0	100	- - -
5000	R0	100	Ch/K, I
5200	R0	100	Ch/K, I
5500	R0	100	Ch/K, I
5700	R0	100	Ch/K, I
6000	R0	50	Ch/K, I
6500	R0	50	Ch/K, I
6700	R0	40	Ch/K, I
7100	R0	40	Ch/K, I

I = illite, Ch/K = chlorite and/or kaolinite
K = kaolinite, Ch = chlorite
Sample # = depth below surface in feet.
All samples are <0.5 micron size cut from cuttings.

TABLE 2. ARCO WELL

Sample	I/S ordering	% Expandability	Accessory Minerals
1000	RO	100	- - -
1200	RO	90	- - -
1500	RO	80	- - -
1800	RO	100	- - -
2100	RO	100	- - -
2900	RO	100	Ch/K, I
3100	RO	80	Ch/K, I
3600	RO	90	Ch/K, I
4200	RO	80	Ch/K, I
4600	RO	80	Ch/K, I
5700	RO	50	Ch/K, I
6600	RO	50	- - -

I = illite, Ch/K = chlorite and/or kaoliinite, K = kaolinite
Ch = chlorite
Sample # = depth below surface in feet.
All samples are <0.5 micron size cut from cuttings.

TABLE 3. LEWIS JOHNSON WELL

Sample	I/S ordering	% Expandability	Accessory Minerals
1500	R0	100	- - -
2700	R0	100	- - -
3700	R0	100	- - -
4400	R0	100	Ch/K, I
5000	R0	95	Ch/K, I
6000	R0	90	Ch/K, I
6200	R0	90	Ch/K, I
6500	R0	100	Ch/K, I
6800	R0	80	Ch/K, I
7000	R0	80	Ch/K, I
7400	R0	100	Ch/K, I
8000	R0 ?	50 ?	Ch/K, I
8400	R0/R1 ?	50 ?	Ch/K, I
9000	R0/R1 ?	50 ?	Ch/K, I
9500	R1	30	Ch/K, I
9700	R1	25	Ch/K, I
9800	R3	18	Ch/K
9900	R3	16	Ch/K

I = illite, Ch/K = chlorite and/or kaolinite, K = kaolinite
Ch = chlorite,
Sample # = depth below surface.
All samples are <0.5 micron size cut from cuttings.
Expandability values for samples 8000, 8400, and 9000 ft. are estimated at 50 percent.

TABLE 4. JACOBSON WELL

Sample	I/S ordering	% Expandability	Accessory Minerals
1000	R0	90	- - -
1500	R0	90	- - -
2500	R0	90	- - -
4500	R0	90	- - -
5500	R0	80	- - -
6000	illite	0	chlorite
6500	illite	0	chlorite
7000	illite	0	chlorite
8000	illite	0	chlorite
8500	illite	0	chlorite
9000	illite	0	chlorite
10500	illite	0	chlorite
11000	illite	0	chlorite

Sample # = depth below surface in feet.
All samples are <0.5 micron size cut from cuttings.

TABLE 5. MONTANA STATE PRISON WELL

Sample	I/S ordering	% Expandability	Accessory Minerals
100	RO	90	I
500	RO	90	I
1000	RO	90	I
1500	RO	90	I
2000	illite	0	Ch/K
2500	illite	0	Ch/K
3000	illite	0	Ch/K
3500	illite	0	Ch
3880	illite	0	Ch
4000	illite	0	Ch
4500	illite	0	Ch
4700	illite	0	Ch
5000	illite	0	Ch
5500	illite	0	Ch
6000	illite	0	Ch
6300	illite	0	Ch

I = illite, Ch/K = chlorite and/or kaolinite
Ch = chlorite,
Sample # = depth below surface in feet.
All samples are <0.5 micron size cut from cuttings.

TABLE 6. HIRSHEY #1 WELL

Sample	I/S ordering	% Expandability	Accessory Minerals
300	R0	100	I, Ch
2410	R0	100	I, Ch
3700	R0	100	I, Ch
4250	R0	100	I, Ch
5180	R0	100	I, Ch
5750	R0	100	I, Ch
6140	R0	100	I, Ch
6560	R1/R2	25	Ch
6970	R1/R2	30	Ch
7480	R1/R2	32	I, Ch
7810	R1/R2	32	Ch
8490	R3	12	- - -
8710	R1/R2	23	Ch
9340	R1/R2	23	Ch
11440	R1/R2	12	Ch
12280	R1	20	Ch
13960	R3	10	Ch
14620	R3	5	Ch
14860	R3	5	Ch, R1 I/S
15790	R3	0	Ch, R1 I/S

I = illite, Ch = chlorite
Sample # = depth below surface in feet.
All samples are <0.5 micron size cut from cuttings.

TABLE 7. HIRSHEY #2 WELL (CUTTINGS)

Sample	I/S ordering	% Expandability	Accessory Minerals
2000	R0	100	- - -
2250	R0	50	- - -
3000	R0	50	- - -
3400	R0	50	- - -
3750	R0	50	- - -
4500	R0	100	I, Ch
5400	R0	50	I, Ch
6200	R0	40	I, Ch
6600	R1	30	I, Ch
6900	R1/R2	30	Ch
7100	R1/R2	30	Ch
7300	R1	30	Ch
7500	R1/R2	30	Ch
7700	R1	28	Ch
8400	illite	0	Ch
8600	illite	0	Ch
8800	R1	20	Ch
11440	R1/R2	20	Ch
12280	R1	20	Ch
13000	R3	10	Ch

I = illite, Ch = chlorite. Sample # = depth below surface in feet. All samples are <0.5 micron size cut from cuttings.

TABLE 8.' HIRSHEY #2 WELL, CORE <0.5 MICRON

Sample	I/S ordering	% Expandability	Accessory Minerals
6564	R1/R2	38	Ch
6565	R1/R2	40	Ch
7576	R1/R2	32	Ch
7589	R1/R2	25	Ch, Fsp
7590	R1/R2	35	Ch, Fsp
7889	R3	13	- - -
7890	R3	18	- - -
7891	R3	13	Ch
7895	R3	20	Fsp
7896	R3	15	Fsp
7902	R3	10	Fsp
7902+	R3	10	- - -
7903	R3	12	- - -
7919	R3	10	- - -
7920	R3	8	- - -
7928	R3	5	Fsp
7940	R3	13	Fsp
7941	R3	15	Fsp
7958	R3	15	- - -
9049	R3	<5	Fsp
10982	ser. + R1/R2	22	Ch, Fsp
10994	ser. + R1	32	Ch, Fsp
11000	ser. + R3	12	Ch, Fsp
11358	ser. + R3	16	Ch, Fsp
11362	ser. + R1	25	Ch, Fsp
11369	ser. + R1/R2	22	Ch, Fsp
11385	ser. + R1	15	Ch, Fsp
11393	ser. + R1	25	Ch, Fsp
11858	ser. + R1	25	Ch, Fsp
11873	ser. + R1/R2	25	Ch, Fsp
11874	ser. + R1/R2	30	Ch, Fsp
11883	ser. + R1	20	Ch, Fsp

Ch = chlorite, Fsp = feldspar (plagioclase or K-feldspar)
ser. = sericite.
Sample # = depth below surface in feet.
See text for discussion of ser. + R1, ser. + R1/R2, and ser. + R3 designations.

TABLE 9. HIRSHEY #2 WELL, CORE <0.1 MICRON

Sample	I/S ordering	% Expandability	Accessory Minerals
6564	R1/R2	50	Ch
6565	R1/R2	50	Ch, Fsp
7576	R1/R2	40	Ch
7589	R1/R2	32	Ch, Fsp
7590	R1/R2	35	Ch, Fsp
7889	R3	20	Fsp
7891	R3	20	Ch
7895	R1/R2	26	- - -
7896	R1	22	- - -
7919	R3	10	- - -
7920	R3	12	- - -
7940	R3	20	- - -
7941	R3	15	- - -
7958	R3	18	Ch, Fsp
9049	ser. + R3	8	Fsp
10982	ser. + R1/R2	30	Ch, Fsp
10994	ser. + R1/R2	25	Ch, Fsp
11000	ser. + R1/R2	26	Ch
11358	ser. + R1	20	Ch, Fsp
11362	ser. + R1	27	Ch, Fsp
11369	ser. + R1	25	Ch, Fsp
11385	ser. + R1/R2	16	Ch, Fsp
11393	ser. + R1/R2	25	Ch, Fsp
11858	ser. + R1/R2	30	Ch
11873	ser. + R1/R2	30	Ch, Fsp
11874	ser. + R1/R2	30	Ch, Fsp
11883	ser. + R1/R2	30	Ch, Fsp

Ch = chlorite, Fsp = feldspar (plagioclase or K-feldspar)
ser. = sericite.
Sample # = depth below surface in feet.
See text for discussion of ser. + R3, ser. + R1/R2, and ser. + R1 designations.

TABLE 10. HIRSHEY #2 CORE SAMPLES

11000 Ft.

Size fraction, in microns.	Illite/smectite ordering and expandability.
< 2.0	ser. + R1 10 % exp.
< 1.0	ser. + R1 ? % exp.
< 0.1	R1 17 % exp.
< 0.05	R1/R2 30 % exp.
< 0.03	R1/R2 25 % exp.
Bracketed size fraction, in microns.	
1.0-2.0	ser. + R1 ? % exp.
0.5-1.0	ser. + R1 ? % exp.
0.1-0.5	ser. + R3 12 % exp.
0.05-0.1	R1/R2 25 % exp.
0.03-0.05	R1/R2 32 % exp.

10982 Ft.

Size fraction, in microns.	
< 0.5	ser. + R1/R2 22 % exp.
< 0.1	ser. + R1/R2 30 % exp.
< 0.05	ser. + R1/R2 32 % exp.

11874 Ft.

< 0.5	ser. + R1/R2 30 % exp.
< 0.1	ser. + R1/R2 30 % exp.
< 0.05	ser. + R1/R2 40 % exp.

XRD results of different size fractions from single samples at 11000, 10982, and 11874 feet from the Hirshey #2 well. See section on mineralogy of different size fractions from single samples, page 12 in text.
ser. = sericite coexisting with illite/smectite

TABLE 11.

Well	Depth in ft. of I/S discont.	% Expand. above discont.	% Expand. below discont.	Change in % expand. at discont.	Depth in ft. and type of unconformity
Benson	5700-6000	100	50	50	5600, Renova/ Lowland Cr.
Arco	4600-5700	80	50	30	5000, Sixmile Cr./Renova
Lewis Johnson	7400-9500	100	30	70	7350, Sixmile Cr./Renova
Jacobson	5500-6000	80	0	80	5700, Low-land Cr./ Cret. shale
Montana State Prison	1500-2000	90	0	90	
Hirshey # 1	6140-6560	100	25	75	
Hirshey # 2	2000-2250	100	50	50	

Depth of I/S discontinuities in cuttings samples compared with percent expandability above and below each discontinuity, change in percent expandability at each discontinuity, and depth and type of unconformity in the Benson, Arco, Lewis Johnson, and Jacobson wells (from McLeod, 1987).